

# Pseudo-Bayesian Robust PCA: Algorithms and Analyses

Tae-Hyun Oh, Yasuyuki Matsushita, In So Kweon and David Wipf

**Abstract**—Commonly used in computer vision and other applications, robust PCA represents an algorithmic attempt to reduce the sensitivity of classical PCA to outliers. The basic idea is to learn a decomposition of some data matrix of interest into low rank and sparse components, the latter representing unwanted outliers. Although the resulting optimization problem is typically NP-hard, convex relaxations provide a computationally-expedient alternative with theoretical support. However, in practical regimes performance guarantees break down and a variety of non-convex alternatives, including Bayesian-inspired models, have been proposed to boost estimation quality. Unfortunately though, without additional a priori knowledge none of these methods can significantly expand the critical operational range such that exact principal subspace recovery is possible. Into this mix we propose a novel pseudo-Bayesian algorithm that explicitly compensates for design weaknesses in many existing non-convex approaches leading to state-of-the-art performance with a sound analytical foundation. Surprisingly, our algorithm can even outperform convex matrix completion despite the fact that the latter is provided with perfect knowledge of which entries are not corrupted.

**Index Terms**—Non-convex robust principal component analysis, variational Bayesian, empirical Bayesian, PCA, matrix completion.



## 1 INTRODUCTION

IT is now well-established that principal component analysis (PCA) is quite sensitive to outliers, with even a single corrupted data element carrying the potential of grossly biasing the recovered principal subspace. This is particularly true in many relevant applications that rely heavily on low-dimensional representations [9], [16], [24], [29], [37]. Mathematically, such outliers can be described by the measurement model  $\mathbf{Y} = \mathbf{Z} + \mathbf{E}$ , where  $\mathbf{Y} \in \mathbb{R}^{n \times m}$  is an observed data matrix,  $\mathbf{Z} = \mathbf{A}\mathbf{B}^T$  is a low-rank component with principal subspace equal to  $\text{span}[\mathbf{A}]$ , and  $\mathbf{E}$  is a matrix of unknown sparse corruptions with arbitrary amplitudes.

Ideally, we would like to remove the effects of  $\mathbf{E}$ , which would then allow regular PCA to be applied to  $\mathbf{Z}$  for obtaining principal components devoid of unwanted bias. For this purpose, robust PCA (RPCA) algorithms have recently been motivated by the optimization problem

$$\min_{\mathbf{Z}, \mathbf{E}} \max(n, m) \cdot \text{rank}[\mathbf{Z}] + \|\mathbf{E}\|_0 \quad \text{s.t. } \mathbf{Y} = \mathbf{Z} + \mathbf{E}, \quad (1)$$

where  $\|\cdot\|_0$  denotes the  $\ell_0$  matrix norm [5] and the  $\max(n, m)$  multiplier ensures that both rank and sparsity terms scale between 0 and  $nm$ , reflecting a priori agnosticism about their relative contributions to  $\mathbf{Y}$ . The basic idea is that if  $\{\mathbf{Z}^*, \mathbf{E}^*\}$  minimizes (1), then  $\mathbf{Z}^*$  is likely to represent the original uncorrupted data.

As a point of reference, if we somehow knew *a priori* which elements of  $\mathbf{E}$  were zero (i.e., no gross corruptions), then (1) could be effectively reduced to the much simpler matrix completion (MC) problem [6]

$$\min_{\mathbf{Z}} \text{rank}[\mathbf{Z}] \quad \text{s.t. } y_{ij} = z_{ij}, \quad \forall (i, j) \in \Omega, \quad (2)$$

where  $\Omega$  denotes the set of indices corresponding with zero-valued elements in  $\mathbf{E}$ . A major challenge with RPCA is that an accurate estimate of the support set  $\Omega$  can be elusive.

Unfortunately, solving (1) is non-convex, discontinuous, and NP-hard in general. Therefore, the convex surrogate referred to as principal component pursuit (PCP)

$$\min_{\mathbf{Z}, \mathbf{E}} \sqrt{\max(n, m)} \cdot \|\mathbf{Z}\|_* + \|\mathbf{E}\|_1 \quad \text{s.t. } \mathbf{Y} = \mathbf{Z} + \mathbf{E} \quad (3)$$

is often adopted, where  $\|\cdot\|_*$  denotes the nuclear norm and  $\|\cdot\|_1$  is the  $\ell_1$  matrix norm. These represent the tightest convex relaxations of the rank and  $\ell_0$  norm functions respectively. Several theoretical results quantify technical conditions whereby the solutions of (1) and (3) are actually equivalent [5], [7]. However, these conditions are highly restrictive and do not provably hold in practical situations of interest such as face clustering [12], motion segmentation [12], high dynamic range imaging [24] or background subtraction [5]. Moreover, both the nuclear and  $\ell_1$  norms are sensitive to data variances, often over-shrinking large singular values of  $\mathbf{Z}$  or coefficients in  $\mathbf{E}$  [13].

All of this motivates stronger approaches to approximating (1). In Section 2 we review existing alternatives, including both non-convex and probabilistic approaches; however, we argue that none of these can significantly outperform PCP in terms of principal subspace recovery in important, representative experimental settings devoid of prior knowledge (e.g., true signal distributions, outlier locations, rank, etc.). We then derive a new pseudo-Bayesian algorithm in Section 3 that has been tailored to conform with principled overarching design criteria. By ‘pseudo’, we mean an algorithm inspired by Bayesian modeling conventions, but with special modifications that deviate from the original probabilistic script for reasons related to estimation quality and computational efficiency. Next, Section 4 examines relevant theoretical properties, explicitly accounting for all approximations involved, while Section 5 provides empirical validations. A preliminary version of this paper has appeared in [25]. We extend [25] by analyzing the behavior of the proposed method in both theoretical with

T.-H. Oh and I. S. Kweon are with the Department of Electrical Engineering, KAIST, Daejeon, South Korea, e-mail: thoh.kaist.ac.kr@gmail.com; iskweon@kaist.ac.kr

Y. Matsushita is with Multimedia Engineering, Graduate School of Information Science and Technology, Osaka University, Japan, e-mail: yasumat@ist.osaka-u.ac.jp

D. Wipf is with Microsoft Research, Beijing, China, e-mail: david-wipf@microsoft.com

proofs and empirical aspects as follows. A detailed proofs on statements are newly supplemented. Additionally, we elucidate the relationship of the proposed method with convex PCP and variational Bayesian robust PCA in Appendix. We also provide detailed derivations and descriptions of an efficient implementation, alternating directional method of multiplier (ADMM), that can improve the performance of the proposed algorithm. Additional simulation and experimental results are included in Section 5. Our high-level contributions can be summarized as follows:

- We derive a new pseudo-Bayesian RPCA algorithm with efficient ADMM subroutine.
- While provable recovery guarantees are completely absent for non-convex RPCA algorithms, we nonetheless quantify how our pseudo-Bayesian design choices lead to a desirable energy landscape. In particular, we show that although any outlier support pattern will represent an inescapable local minima of (1) (or a broad class of functions that mimic (1)), our proposal can simultaneously retain the correct global optimum while eradicating at least some of the suboptimal minima associated with incorrect outlier location estimates.
- We empirically demonstrate improved performance over state-of-the-art algorithms (including PCP) in terms of standard phase transition plots with a dramatically expanded success region. Quite surprisingly, our algorithm can even outperform convex matrix completion (MC) despite the fact that the latter is provided with *perfect knowledge of which entries are not corrupted*, suggesting that robust outlier support pattern estimation is indeed directly facilitated by our model.

## 2 RECENT WORK

The vast majority of algorithms for solving (1) either implicitly or explicitly attempt to solve a problem of the form

$$\min_{\mathbf{Z}, \mathbf{E}} f_1(\mathbf{Z}) + \sum_{i,j} f_2(e_{ij}) \quad \text{s.t. } \mathbf{Y} = \mathbf{Z} + \mathbf{E}, \quad (4)$$

where  $f_1$  and  $f_2$  are penalty functions that favor minimal rank and sparsity respectively. When  $f_1$  is the nuclear norm (scaled appropriately) and  $f_2(e) = |e|$ , then (4) reduces to (3). Methods differ however by replacing  $f_1$  and  $f_2$  with non-convex alternatives, such as generalized Huber functions (Hub-RPCA) [8] or Schatten  $\ell_p$  quasi-norms with  $p < 1$  (Sch-RPCA) [20], [21]. When applied to the singular values of  $\mathbf{Z}$  and elements of  $\mathbf{E}$  respectively, these selections enact stronger enforcement of minimal rank and sparsity. If prior knowledge of the true rank of  $\mathbf{Z}$  is available, a truncated nuclear norm approach (TNN-RPCA) has also been proposed [26]. Further divergences follow from the spectrum of optimization schemes applied to different objectives, such as the alternating directions method of multipliers (ADMM) algorithm [4] or iteratively reweighted least squares (IRLS) [20].

With all of these methods, we may consider relaxing the strict equality constraint to the regularized form

$$\min_{\mathbf{Z}, \mathbf{E}} \frac{1}{\lambda} \|\mathbf{Y} - \mathbf{Z} - \mathbf{E}\|_{\mathcal{F}}^2 + f_1(\mathbf{Z}) + \sum_{i,j} f_2(e_{ij}), \quad (5)$$

where  $\lambda > 0$  is a trade-off parameter. This has inspired a number of competing Bayesian formulations, which typically proceed as follows. Let

$$p(\mathbf{Y}|\mathbf{Z}, \mathbf{E}) \propto \exp \left[ -\frac{1}{2\lambda} \|\mathbf{Y} - \mathbf{Z} - \mathbf{E}\|_{\mathcal{F}}^2 \right] \quad (6)$$

define a likelihood function, where  $\lambda$  represents a non-negative variance parameter assumed to be known.<sup>1</sup> Hierarchical prior distributions are then assigned to  $\mathbf{Z}$  and  $\mathbf{E}$  to encourage minimal rank and strong sparsity, respectively. For the latter, the most common choice is the Gaussian scale-mixture (GSM) defined hierarchically by

$$p(\mathbf{E}|\mathbf{\Gamma}) = \prod_{i,j} p(e_{ij}|\gamma_{ij}), \quad p(e_{ij}|\gamma_{ij}) \propto \exp \left[ -\frac{e_{ij}^2}{2\gamma_{ij}} \right], \quad (7)$$

with hyper prior,  $p(\gamma_{ij}^{-1}) \propto \gamma_{ij}^{1-a} \exp[-\frac{b}{\gamma_{ij}}]$ , where  $\mathbf{\Gamma}$  is a matrix of non-negative variances and  $a, b \geq 0$  are fixed parameters. Note that when these values are small, the resulting distribution over each  $e_{ij}$  (obtained by marginalizing over the respective  $\gamma_{ij}$ ) is heavy-tailed with a sharp peak at zero, the defining characteristics of sparse priors.

For the prior on  $\mathbf{Z}$ , Bayesian methods have somewhat broader distinctions. Particularly, a number of methods explicitly assume that  $\mathbf{Z} = \mathbf{A}\mathbf{B}^\top$  and specify GSM priors on  $\mathbf{A}$  and  $\mathbf{B}$  [1], [11], [33]. For example, variational Bayesian RPCA (VB-RPCA) [1] assumes  $p(\mathbf{A}|\boldsymbol{\theta}) \propto \exp[-\text{tr}(\mathbf{A} \text{diag}[\boldsymbol{\theta}]^{-1} \mathbf{A}^\top)]$ , where  $\boldsymbol{\theta}$  is a non-negative variance vector. An equivalent prior is used for  $p(\mathbf{B}|\boldsymbol{\theta})$  with a shared value of  $\boldsymbol{\theta}$ . This model also applies the prior  $p(\boldsymbol{\theta}) = \prod_i p(\theta_i)$  with  $p(\theta_i)$  defined for consistency with  $p(\gamma_{ij}^{-1})$  in Eq. (7). Low rank solutions are favored via the same mechanism as described above for sparsity, but only the sparse variance prior is applied to *columns* of  $\mathbf{A}$  and  $\mathbf{B}$ , effectively pruning them from the model if the associated  $\theta_i$  is small. Given the above, the joint distribution is

$$p(\mathbf{Y}, \mathbf{A}, \mathbf{B}, \mathbf{E}, \mathbf{\Gamma}, \boldsymbol{\theta}) = p(\mathbf{Y}|\mathbf{A}, \mathbf{B}, \mathbf{E})p(\mathbf{E}|\mathbf{\Gamma})p(\mathbf{A}|\boldsymbol{\theta})p(\mathbf{B}|\boldsymbol{\theta})p(\mathbf{\Gamma})p(\boldsymbol{\theta}). \quad (8)$$

Full Bayesian inference with this is intractable, hence a common variational Bayesian (VB) mean-field approximation is applied [1], [3]. The basic idea is to obtain a tractable approximate factorial posterior distribution by solving

$$\min_{q(\Phi)} \mathcal{KL}[q(\Phi)||p(\mathbf{A}, \mathbf{B}, \mathbf{E}, \mathbf{\Gamma}, \boldsymbol{\theta}|\mathbf{Y})], \quad (9)$$

where  $q(\Phi) \triangleq q(\mathbf{A})q(\mathbf{B})q(\mathbf{E})q(\mathbf{\Gamma})q(\boldsymbol{\theta})$ , each  $q$  represents an arbitrary probability distribution, and  $\mathcal{KL}[\cdot||\cdot]$  denotes the Kullback-Leibler divergence between two distributions. This can be accomplished via coordinate descent minimization over each respective  $q$  distribution while holding the others fixed. Final estimates of  $\mathbf{Z}$  and  $\mathbf{E}$  are obtained by the means of  $q(\mathbf{A})$ ,  $q(\mathbf{B})$ , and  $q(\mathbf{E})$  upon convergence. A related hierarchical model is used in [11], [33], but MCMC sampling techniques are used for full Bayesian inference RPCA (FB-RPCA) at the expense of considerable computational complexity and multiple tuning parameters.

An alternative empirical Bayesian algorithm (EB-RPCA) is described in [34]. In addition to the likelihood function (6) and prior from (7), this method assumes a direct Gaussian prior on  $\mathbf{Z}$  given by

$$p(\mathbf{Z}|\Psi) \propto \exp \left[ -\frac{1}{2} \text{tr} \left( \mathbf{Z}^\top \Psi^{-1} \mathbf{Z} \right) \right], \quad (10)$$

1. Actually many methods attempt to learn this parameter from data, but we avoid this consideration for simplicity. As well, for subtle reasons such learning is sometimes not even identifiable in the strict statistical sense.

where  $\Psi$  is a symmetric and positive definite matrix.<sup>2</sup> Inference is accomplished via an empirical Bayesian approach [22]. The basic idea is to marginalize out the unknown  $\mathbf{Z}$  and  $\mathbf{E}$  and solve

$$\max_{\Psi, \Gamma} \iint p(\mathbf{Y}|\mathbf{Z}, \mathbf{E})p(\mathbf{Z}|\Psi)p(\mathbf{E}|\Gamma)d\mathbf{Z}d\mathbf{E} \quad (11)$$

using an EM-like algorithm. Once we have an optimal  $\{\Psi^*, \Gamma^*\}$ , we then compute the posterior mean of  $p(\mathbf{Z}, \mathbf{E}|\mathbf{Y}, \Psi^*, \Gamma^*)$  which is available in closed-form.

Finally, a recent class of methods has been derived around the concept of approximate message passing, AMP-RPCA [28], which applies Gaussian priors to the factors  $\mathbf{A}$  and  $\mathbf{B}$ , and infers posterior estimates by loopy belief propagation [23]. In our experiments, we found AMP-RPCA to be quite sensitive to data deviating from these distributions.

### 3 A NEW PSEUDO-BAYESIAN ALGORITHM

As it turns out, it is quite difficult to derive a fully Bayesian model, or some tight variational/empirical approximation, that leads to an efficient algorithm capable of consistently outperforming the original convex PCP, at least in the absence of additional, exploitable prior knowledge. It is here that we adopt a pseudo-Bayesian approach, by which we mean that a Bayesian-inspired cost function will be altered using manipulations that, although not consistent with any original Bayesian model, nonetheless produce desirable attributes relevant to blindly solving (1). In some sense however, we view this as a strength, because the final model analysis presented later in Section 4 does not rely on any presumed validity of the underlying prior assumptions, but rather on explicit properties of the objective that emerges, including all assumptions and approximation involved.

#### 3.1 Algorithm Derivation

**Basic Model:** We begin with the same likelihood function from (6), noting that in the limit as  $\lambda \rightarrow 0$  this will enforce the constraint set from (1). We also adopt the same prior on  $\mathbf{E}$  given by (7) above and used in [1] and [34], but we need not assume any additional hyperprior on  $\Gamma$ . In contrast, for the prior on  $\mathbf{Z}$  our method diverges, and we define the Gaussian

$$p(\mathbf{Z}|\Psi_r, \Psi_c) \propto \exp\left[-\frac{1}{2}\bar{\mathbf{z}}^\top (\Psi_r \otimes \mathbf{I} + \mathbf{I} \otimes \Psi_c)^{-1} \bar{\mathbf{z}}\right], \quad (12)$$

where  $\bar{\mathbf{z}} \triangleq \text{vec}[\mathbf{Z}]$  is the column-wise vectorization of  $\mathbf{Z}$ ,  $\otimes$  denotes the Kronecker product, and  $\Psi_c \in \mathbb{R}^{n \times n}$  and  $\Psi_r \in \mathbb{R}^{m \times m}$  are positive semi-definite, symmetric matrices.<sup>3</sup> Here  $\Psi_c$  can be viewed as applying a column-wise covariance factor, and  $\Psi_r$  a row-wise one. Note that if  $\Psi_r = 0$ , then this prior collapses to (10); however, by including  $\Psi_r$  we can retain symmetry in our model, or invariance to inference using either  $\mathbf{Y}$  or  $\mathbf{Y}^\top$ . Related priors can also be used to improve the performance of affine rank minimization problems [38].

2. Note that in [34] this method is motivated from an entirely different variational perspective anchored in convex analysis; however, the cost function that ultimately emerges is equivalent to what follows with these priors.

3. Technically the Kronecker sum  $\Psi_r \otimes \mathbf{I} + \mathbf{I} \otimes \Psi_c$  must be positive definite for the inverse in (12) to be defined. However, we can accommodate the semi-definite case using the following convention. Without loss of generality assume that  $\Psi_r \otimes \mathbf{I} + \mathbf{I} \otimes \Psi_c = \mathbf{R}\mathbf{R}^\top$  for some matrix  $\mathbf{R}$ . We then qualify that  $p(\mathbf{Z}|\Psi_r, \Psi_c) = 0$  if  $\bar{\mathbf{z}} \notin \text{span}[\mathbf{R}]$ , and  $p(\mathbf{Z}|\Psi_r, \Psi_c) \propto \exp[-\frac{1}{2}\bar{\mathbf{z}}^\top (\mathbf{R}^\top)^\dagger \mathbf{R}^\dagger \bar{\mathbf{z}}]$  otherwise.

We apply the empirical Bayesian procedure from (11); the resulting convolution of Gaussians integral [3] can be computed in closed-form. After applying  $-2\log[\cdot]$  transformation, this is equivalent to minimizing

$$\mathcal{L}(\Psi_r, \Psi_c, \Gamma) = \bar{\mathbf{y}}^\top \Sigma_y^{-1} \bar{\mathbf{y}} + \log |\Sigma_y|, \quad (13)$$

where  $\Sigma_y \triangleq \Psi_r \otimes \mathbf{I} + \mathbf{I} \otimes \Psi_c + \bar{\Gamma} + \lambda \mathbf{I}$ ,

and  $\bar{\Gamma} \triangleq \text{diag}[\bar{\gamma}]$ . Note that for even reasonably sized problems  $\Sigma_y \in \mathbb{R}^{nm \times nm}$  will be huge, and consequently we will require certain approximations to produce affordable update rules. Fortunately this can be accomplished while simultaneously retaining a principled objective function capable of outperforming existing methods.

**Pseudo-Bayesian Objective:** We first modify (13) to give

$$\mathcal{L}(\Psi_r, \Psi_c, \Gamma) = \bar{\mathbf{y}}^\top \Sigma_y^{-1} \bar{\mathbf{y}} + \sum_j \log |\Psi_c + \frac{1}{2}\Gamma_{.j} + \frac{\lambda}{2}\mathbf{I}| + \sum_i \log |\Psi_r + \frac{1}{2}\Gamma_{i.} + \frac{\lambda}{2}\mathbf{I}|, \quad (14)$$

where  $\Gamma_{.j} \triangleq \text{diag}[\gamma_{.j}]$  and  $\gamma_{.j}$  represents the  $j$ -th column of  $\Gamma$ . Similarly we define  $\Gamma_{i.} \triangleq \text{diag}[\gamma_{i.}]$  with  $\gamma_{i.}$  the  $i$ -th row of  $\Gamma$ . This new cost is nothing more than (13) but with the  $\log|\cdot|$  term split in half producing a lower bound by Jensen's inequality; the Kronecker product can naturally be dissolved under these conditions. Additionally, (14) represents a departure from our original Bayesian model in that there is no longer any direct empirical Bayesian or VB formulation that would lead to (14). Note that although this modification cannot be justified on strictly probabilistic terms, we will see shortly that it nonetheless still represents a viable cost function in the abstract sense, and lends itself to increased computational efficiency. The latter is an immediate effect of the drastically reduced dimensionality of the matrices inside the determinant. Henceforth (14) will represent the cost function that we seek to minimize; relevant properties will be handled in Section 4. We emphasize that all subsequent analysis in Section 4 is based directly upon (14), and therefore already accounts for the approximation step in advancing from (13). This is unlike other Bayesian model justifications relying on the legitimacy of the original full model, and yet then adopt various approximations that may completely change the problem.

**Update Rules:** Common to many empirical Bayesian and VB approaches, our basic optimization strategy involves iteratively optimizing upper bounds on (14) in the spirit of majorization-minimization [15]. At a high level, our goal will be to apply bounds which separate  $\Psi_c$ ,  $\Psi_r$ , and  $\Gamma$  into terms of the general form  $\log|\mathbf{X}| + \text{tr}[\mathbf{A}\mathbf{X}^{-1}]$ , the reason being that this expression has a simple global minimum over  $\mathbf{X}$  given by  $\mathbf{X} = \mathbf{A}$ . Therefore the strategy will be to update the bound (parameterized by some matrix  $\mathbf{A}$ ), and then update the parameters of interest  $\mathbf{X}$ .

Using standard conjugate duality relationships and variational bounding techniques [17][Chapter 4], it follows after some linear algebra that

$$\bar{\mathbf{y}}^\top \Sigma_y^{-1} \bar{\mathbf{y}} \leq \frac{1}{\lambda} \|\mathbf{Y} - \mathbf{Z} - \mathbf{E}\|_{\mathcal{F}}^2 + \sum_{i,j} \frac{e_{ij}^2}{\gamma_{ij}} + \bar{\mathbf{z}}^\top (\Psi_r \otimes \mathbf{I} + \mathbf{I} \otimes \Psi_c)^{-1} \bar{\mathbf{z}} \quad (15)$$

for all  $\mathbf{Z}$  and  $\mathbf{E}$ . For fixed values of  $\Psi_r$ ,  $\Psi_c$ , and  $\Gamma$  we optimize this quadratic bound to obtain revised estimates for  $\mathbf{Z}$  and  $\mathbf{E}$ ,

noting that exact equality in (15) is possible via the closed-form solution

$$\begin{aligned}\bar{\mathbf{z}} &= (\Psi_r \otimes \mathbf{I} + \mathbf{I} \otimes \Psi_c) \Sigma_y^{-1} \bar{\mathbf{y}}, \\ \bar{\mathbf{e}} &= \bar{\Gamma} \Sigma_y^{-1} \bar{\mathbf{y}}.\end{aligned}\quad (16)$$

In large practical problems, (16) may become expensive to compute directly because of the high dimensional inverse involved. However, we can still find the optimum efficiently by an ADMM procedure described in Appendix.

We can also further bound the righthand side of (15) using Jensen's inequality as

$$\bar{\mathbf{z}}^\top (\Psi_r \otimes \mathbf{I} + \mathbf{I} \otimes \Psi_c)^{-1} \bar{\mathbf{z}} \leq \text{tr} \left[ \mathbf{Z}^\top \mathbf{Z} \Psi_r^{-1} + \mathbf{Z} \mathbf{Z}^\top \Psi_c^{-1} \right]. \quad (17)$$

Along with (15) this implies that for fixed values of  $\mathbf{Z}$  and  $\mathbf{E}$  we can obtain an upper bound which only depends on  $\Psi_r$ ,  $\Psi_c$ , and  $\Gamma$  in a decoupled or separable fashion.

For the  $\log |\cdot|$  terms in (14), we also derive convenient upper bounds using determinant identities and a first-order approximation, the goal being to find a representation that plays well with the previous decoupled bound for optimization purposes. Again using conjugate duality relationships, we can form the bound

$$\begin{aligned}\log \left| \Psi_c + \frac{1}{2} \Gamma_{\cdot j} + \frac{\lambda}{2} \mathbf{I} \right| &\equiv \log |\Psi_c| + \log |\Gamma_{\cdot j}| + \log |W(\Psi_c, \Gamma_{\cdot j})| \\ &\leq \log |\Psi_c| + \log |\Gamma_{\cdot j}| + \text{tr} \left[ (\nabla_{\Psi_c^{-1}}^j)^\top \Psi_c^{-1} \right] \\ &\quad + (\nabla_{\Gamma_{\cdot j}^{-1}}^c)^\top \gamma_{\cdot j}^{-1} + C,\end{aligned}\quad (18)$$

where the inverse  $\gamma_{\cdot j}^{-1}$  is understood to apply element-wise, and  $W(\Psi_c, \Gamma_{\cdot j})$  is defined as

$$W(\Psi_c, \Gamma_{\cdot j}) \triangleq \frac{1}{2\lambda} \begin{bmatrix} 2\mathbf{I} & \sqrt{2}\mathbf{I} \\ \sqrt{2}\mathbf{I} & \mathbf{I} \end{bmatrix} + \begin{bmatrix} \Psi_c^{-1} & \mathbf{0} \\ \mathbf{0} & \Gamma_{\cdot j}^{-1} \end{bmatrix}. \quad (19)$$

Additionally,  $C$  is a standard constant, which accompanies the first-order approximation to guarantee that the upper bound is tangent to the underlying cost function; however, its exact value is irrelevant for optimization purposes. Finally, the requisite gradients are defined as

$$\begin{aligned}\nabla_{\Gamma_{\cdot j}^{-1}}^c &\triangleq \frac{\partial W(\Psi_c, \Gamma_{\cdot j})}{\partial \Gamma_{\cdot j}^{-1}} = \text{diag}[\Gamma_{\cdot j} - \frac{1}{2} \Gamma_{\cdot j} (\mathbf{S}_c^j)^{-1} \Gamma_{\cdot j}], \\ \nabla_{\Psi_c^{-1}}^j &\triangleq \frac{\partial W(\Psi_c, \Gamma_{\cdot j})}{\partial \Psi_c^{-1}} = \Psi_c - \Psi_c (\mathbf{S}_c^j)^{-1} \Psi_c,\end{aligned}\quad (20)$$

$$\begin{aligned}\nabla_{\Gamma_{i \cdot}^{-1}}^r &\triangleq \frac{\partial W(\Psi_r, \Gamma_{i \cdot}^{-1})}{\partial \Gamma_{i \cdot}^{-1}} = \text{diag} \left[ \Gamma_{i \cdot} - \frac{1}{2} \Gamma_{i \cdot} (\mathbf{S}_r^i)^{-1} \Gamma_{i \cdot} \right], \\ \nabla_{\Psi_r^{-1}}^i &\triangleq \frac{\partial W(\Psi_r, \Gamma_{i \cdot}^{-1})}{\partial \Psi_r^{-1}} = \Psi_r - \Psi_r (\mathbf{S}_r^i)^{-1} \Psi_r,\end{aligned}\quad (21)$$

where  $\mathbf{S}_c^j \triangleq \Psi_c + \frac{1}{2} \Gamma_{\cdot j} + \frac{\lambda}{2} \mathbf{I}$  and  $\mathbf{S}_r^i \triangleq \Psi_r + \frac{1}{2} \Gamma_{i \cdot} + \frac{\lambda}{2} \mathbf{I}$ .

These bounds are principally useful because all  $\Psi_c$ ,  $\Psi_r$ ,  $\Gamma_{\cdot j}$ , and  $\Gamma_{i \cdot}$  factors have been decoupled. Consequently, with  $\mathbf{Z}$ ,  $\mathbf{E}$ , and all the relevant gradients fixed, we can separately combine  $\Psi_c$ ,  $\Psi_r$ , and  $\Gamma$ -dependent terms from the bounds and then optimize independently. For example, combining terms from (17) and (18) involving  $\Psi_c$  for all  $j$ , this requires solving

$$\min_{\Psi_c} m \log |\Psi_c| + \text{tr} \left[ \sum_j (\nabla_{\Psi_c^{-1}}^j)^\top \Psi_c^{-1} + \mathbf{Z} \mathbf{Z}^\top \Psi_c^{-1} \right]. \quad (22)$$

Analogous cost functions emerge for  $\Psi_r$  and  $\Gamma$ . All three problems have closed-form optimal solutions given by

$$\begin{aligned}\Psi_c &= \frac{1}{m} \left[ \sum_j \nabla_{\Psi_c^{-1}}^j + \mathbf{Z} \mathbf{Z}^\top \right], \\ \Psi_r &= \frac{1}{n} \left[ \sum_i \nabla_{\Psi_r^{-1}}^i + \mathbf{Z}^\top \mathbf{Z} \right], \\ \bar{\gamma} &= \bar{\mathbf{z}}^2 + \bar{\mathbf{u}}_c + \bar{\mathbf{u}}_r,\end{aligned}\quad (23)$$

where the squaring operator is applied element-wise to  $\bar{\mathbf{z}}$ ,  $\bar{\mathbf{u}}_c \triangleq [\nabla_{\Gamma_{\cdot 1}^{-1}}^c; \dots; \nabla_{\Gamma_{\cdot m}^{-1}}^c]$ , and analogously for  $\bar{\mathbf{u}}_r$ . One interesting aspect of (23) is that it forces  $\Psi_c \succeq \frac{1}{m} \mathbf{Z} \mathbf{Z}^\top$  and  $\Psi_r \succeq \frac{1}{n} \mathbf{Z}^\top \mathbf{Z}$ , thus maintaining a balancing symmetry and preventing one or the other from possibly converging towards zero. This is another desirable consequence of using the bound in (17). To finalize then, the proposed pipeline, which we henceforth refer to as pseudo-Bayesian RPCA (PB-RPCA), involves the steps shown under Algorithm 1. These can be implemented in such a way that (14) is guaranteed to be reduced or left unchanged at each step, with complexity linear in  $\max(n, m)$  and cubic in  $\min(n, m)$ .

In summary, the pseudo-code of PB-RPCA procedure is presented as Algorithm 1.

---

#### Algorithm 1 Pseudo-Bayesian Robust PCA.

---

**Input :** Observation matrix  $\mathbf{Y} \in \mathbb{R}^{n \times m}$ , and  $\lambda > 0$ .

Initialize  $\Psi_c = \mathbf{I}$ ,  $\Psi_r = \mathbf{I}$ ,  $\Gamma$  to a matrix of ones, and  $\mathbf{Z} = \mathbf{E} = \mathbf{0}$ .

**repeat**

    Compute (16) using ADMM or sparse matrix routines if necessary.

    Compute the gradients  $\nabla_{\Psi_c^{-1}}^j, \nabla_{\Psi_r^{-1}}^i, \nabla_{\Gamma_{\cdot j}^{-1}}^c$  and  $\nabla_{\Gamma_{i \cdot}^{-1}}^r$  as in (20) and (21).

    Update  $\Psi_c$ ,  $\Psi_r$ , and  $\Gamma$  using (23).

**until** convergence.

**Output :** Final estimate for  $\mathbf{Z}$  and  $\mathbf{E}$  coming from (16).

---

## 4 ANALYSIS OF THE PB-RPCA OBJECTIVE

On the surface it may appear that the PB-RPCA objective (14) represents a rather circuitous route to solving (1), with no obvious advantage over the convex PCP relaxation from (3), or any other approach for that matter. However quite surprisingly, we prove (later will be shown in Appendix) that by simply replacing the  $\log |\cdot|$  matrix operators in (14) with  $\text{tr}[\cdot]$ , the resulting function collapses exactly to convex PCP. So what at first appear as distant cousins are actually quite closely related objectives. Of course our work is still in front of us to explain why  $\log |\cdot|$ , and therefore the PB-RPCA objective by association, might display any particular advantage. This leads us to considerations of *relative concavity*, *non-separability*, and *symmetry* as described below in turn.

**Relative Concavity:** Although both  $\log |\cdot|$  and  $\text{tr}[\cdot]$  are concave non-decreasing functions of the singular values of symmetric positive definite matrices, and hence favor both sparsity of  $\Gamma$  and minimal rank of  $\Psi_r$  or  $\Psi_c$ , the former is far more strongly concave (in the sense of relative concavity described in [27]). In this respect we may expect that  $\log |\cdot|$  is less likely to over-shrink large values [13]. Moreover, applying a concave non-decreasing penalty to elements of  $\Gamma$  favors a sparse estimate, which in turn transfers this sparsity directly to  $\mathbf{E}$  by virtue of

the left multiplication by  $\bar{\Gamma}$  in (16). Likewise for the singular values of  $\Psi_c$  and  $\Psi_r$ .

**Non-Separability:** While potentially desirable, the relative concavity distinction described above is certainly not sufficient to motivate why PB-RPCA might represent an effective RPCA approach, especially given the breadth of non-convex alternatives already in the literature. However, a much stronger argument can be made by exposing a fundamental limitation of all RPCA methods (convex or otherwise) that rely on minimization of generic penalties in the separable or additive form of (4). For this purpose, let  $\Omega$  denote a set of indices that correspond with zero-valued elements in  $\mathbf{E}$ , such that  $\mathbf{E}_\Omega = 0$  while all other elements of  $\mathbf{E}$  are arbitrary nonzeros (it can equally be viewed as the complement of the support of  $\mathbf{E}$ ). In the case of MC,  $\Omega$  would also represent the set of observed matrix elements. We then have the following:

**Proposition 1.** *To guarantee that (4) has the same global optimum as (1) for all  $\mathbf{Y}$  where a unique solution exists, it follows that  $f_1$  and  $f_2$  must be non-convex and no feasible descent direction can ever remove an index from or decrease the cardinality of  $\Omega$ .*

In [34] it has been shown that, under similar conditions, the gradient in a feasible direction at any zero-valued element of  $\mathbf{E}$  must be infinite to guarantee a matching global optimum, from which this result naturally follows. The ramifications of this proposition are profound if we ever wish to produce a version of RPCA that can mimic the desirable behavior of much simpler MC problems with known support, or at least radically improve upon PCP with unknown outlier support. In words, Proposition 1 implies that under the stated global-optimality preserving conditions, if any element of  $\mathbf{E}$  converges to zero during optimization with an arbitrary descent algorithm, it will remain anchored at zero until the end. Consequently, if the algorithm prematurely errs in setting the wrong element to zero, meaning the wrong support pattern has been inferred at *any* time during an optimization trajectory, it is impossible to ever recover, a problem naturally side-stepped by MC where the support is effectively known. Therefore, the adoption of separable penalty functions can be quite constraining and they are unlikely to produce sufficiently reliable support recovery.

But how does this relate to PB-RPCA? Our algorithm maintains a decidedly *non-separable* penalty function on  $\Psi_c$ ,  $\Psi_r$ , and  $\Gamma$ , which directly transfers to an implicit, non-separable regularizer over  $\mathbf{Z}$  and  $\mathbf{E}$  when viewed through the dual-space framework from [35].<sup>4</sup> By this we mean a penalty  $f(\mathbf{Z}, \mathbf{E}) \neq f_1(\mathbf{Z}) + f_2(\mathbf{E})$  for any functions  $f_1$  and  $f_2$ , and with  $\mathbf{Z}$  fixed, we have  $f(\mathbf{Z}, \mathbf{E}) \neq \sum_{i,j} f_{ij}(e_{ij})$  for any set of functions  $\{f_{ij}\}$ .

We now examine the consequences. Let  $\Omega$  now denote a set of indices that correspond with zero-valued elements in  $\Gamma$ , which translates into an equivalent support set for  $\mathbf{Z}$  via (16). This then leads to quantifiable benefits:

**Proposition 2.** *The following properties hold w.r.t. the PB-RPCA objective (assuming  $n = m$  for simplicity):*

- Assume that a unique global solution to (1) exists such that either  $\text{rank}[\mathbf{Z}] + \max_j \|e_{\cdot j}\|_0 < n$  or  $\text{rank}[\mathbf{Z}] + \max_i \|e_i\|_0 < n$ . Additionally, let  $\{\Psi_c^*, \Psi_r^*, \Gamma^*\}$  denote a globally minimizing solution to (14) and  $\{\mathbf{Z}^*, \mathbf{E}^*\}$  the corresponding values of  $\mathbf{Z}$

4. Even though this penalty function is not available in closed-form, non-separability is nonetheless enforced via the linkage between  $\Psi_c$ ,  $\Psi_r$ , and  $\Gamma$  in the  $\log|\cdot|$  operator.

and  $\mathbf{E}$  computed using (16). Then in the limit  $\lambda \rightarrow 0$ ,  $\mathbf{Z}^*$  and  $\mathbf{E}^*$  globally minimize (1).

- Assume that  $\mathbf{Y}$  has no entries identically equal to zero.<sup>5</sup> Then for any arbitrary  $\Omega$ , there will always exist a range of  $\Psi_c$  and  $\Psi_r$  values such that for any  $\Gamma$  consistent with  $\Omega$  we are not at a locally minimizing solution to (14), meaning there exists a feasible descent direction whereby elements of  $\Gamma$  can escape from zero.

A couple important comments are worth stating regarding this result. First, the rank and row/column-sparsity requirements are extremely mild. In fact, *any* minimum of (1) will be such that  $\text{rank}[\mathbf{Z}] + \max_j \|e_{\cdot j}\|_0 \leq n$  and  $\text{rank}[\mathbf{Z}] + \max_i \|e_i\|_0 \leq m$ , regardless of  $\mathbf{Y}$ . Secondly, unlike *any* separable penalty function (4) that retains the correct global optimal as (1), Proposition 2 implies that (14) need not be locally minimized by every possible support pattern for outlier locations. Consequently, premature convergence to suboptimal supports need not disrupt trajectories towards the global solution to the extent that (4) may be obstructed. Moreover, beyond algorithms that explicitly adopt separable penalties (the vast majority), some existing Bayesian approaches may implicitly default to (4). For example, the mean-field factorizations adopted by VB-RPCA actually allow the underlying free energy objective to be expressible as (4) for some  $f_1$  and  $f_2$  as will be shown in Appendix.

**Symmetry:** Without the introduction of symmetry via our pseudo-Bayesian proposal (meaning either  $\Psi_c$  or  $\Psi_r$  is forced to zero), then PB-RPCA collapses to something like EB-RPCA, which depends heavily on whether  $\mathbf{Y}$  or  $\mathbf{Y}^\top$  is provided as input and penalizes column- and row-spaces asymmetrically. In this regime it can be shown that the analogous requirement to replicate Proposition 2 becomes more stringent, namely we must assume the asymmetric condition  $\text{rank}[\mathbf{Z}] + \max_j \|e_{\cdot j}\|_0 < n$ . Thus the symmetric cost of PB-RPCA of allows us to relax this column-wise restriction provided a row-wise alternative holds (and vice versa), allowing the PB-RPCA objective (14) to match the global optimum of our original problem from (1) under broader conditions.

In closing this section, we reiterate that all of our analysis and conclusions are based on (14), *after* the stated approximations. Therefore we need not rely on the plausibility of the original Bayesian starting point from Section 3 nor the tightness of subsequent approximations for justification; rather (14) can be viewed as a principled stand-alone objective for RPCA regardless of its origins. Moreover, it represents the first approach satisfying the relative concavity, non-separability, and symmetry properties described above, which can loosely be viewed as necessary, but not sufficient design criteria for an optimal RPCA objective.

## 5 EXPERIMENTS

To examine significant factors that influence the ability to solve (1), we first evaluate the relative performance of PB-RPCA estimating random simulated subspaces from corrupted measurements, the standard benchmark. Later we present subspace clustering results for motion segmentation and a photometric stereo example as practical applications.

**Settings and Parameters** We set parameters based on the values suggested by original authors with one exception,

5. This assumption can be relaxed with some additional effort but we avoid such considerations here for clarity of presentation.

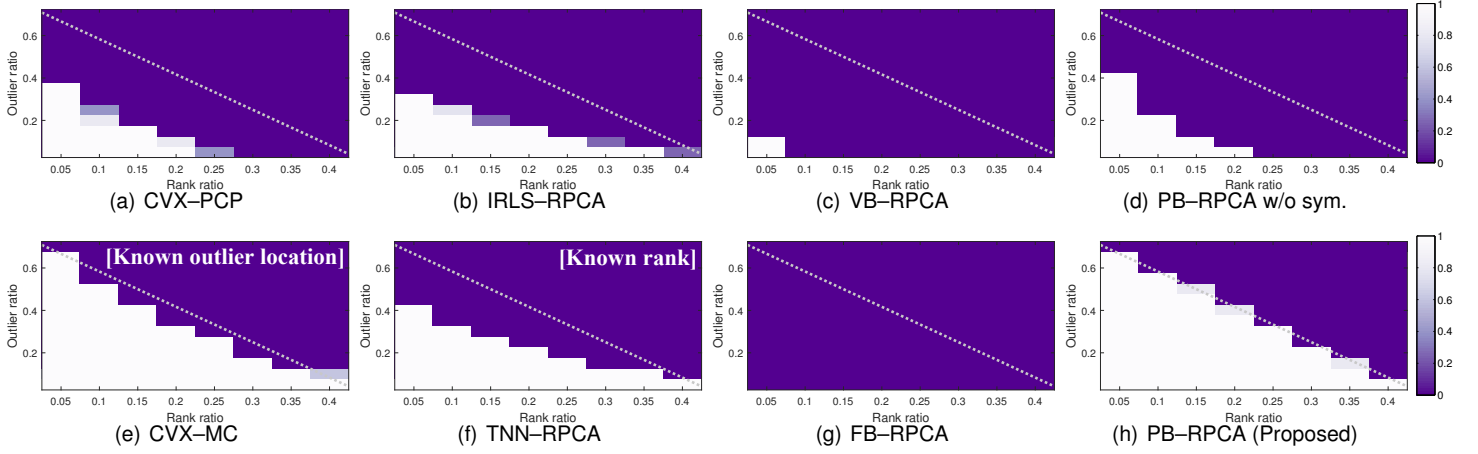


Fig. 1. Phase transition over outlier (y-axis) and rank (x-axis) ratio variations. Experiments with  $\text{NRMSE} < 0.001$  are regarded as success. Here CVX-MC and TNN-RPCA maintain advantages of exactly known outlier support pattern and true rank respectively. Brighter color represents better performance.

IRLS [20]. The published code of IRLS only supports Schatten- $p$  norm and  $\ell_{2,q}$ -norm minimization with an affine constraint. Consequently, we have modified to accommodate the RPCA algorithm (a straightforward adaptation). Since the parameters used in the original code are no longer suitable for RPCA, we tuned them to make the algorithm stable and achieve the best performance. For objective function parameters, we used the Schatten  $p$ -norm and  $\ell_q$ -norm with  $p=q=0.01$ , and  $\lambda=1/\sqrt{\max(n,m)}$ . For embedded optimization parameters, we used  $\epsilon=10^{-6}$ ,  $\rho=1.05$  and  $\mu=0.1\|\mathbf{X}\|_2$ , with context and notation deferred to [20].

## 5.1 Phase Transition Graphs

We compare our method against existing RPCA methods: PCP [18], TNN [26], IRLS [20], VB [1], and FB [11]. AMP [28]. We also include results using PB-RPCA but with symmetry removed (which then defaults to something like EB-RPCA), allowing us to isolate the importance of this factor, called ‘‘PB-RPCA w/o sym.’’. For competing algorithms, we set parameters based on the values suggested by original authors with the exception of IRLS.

We construct phase transition plots as in [5], [11] that evaluate the recovery success of every pairing of outlier ratio and rank using data  $\mathbf{Y}=\mathbf{Z}_{GT}+\mathbf{E}_{GT}$ , where  $\mathbf{Y}\in\mathbb{R}^{m\times n}$  and  $m=n=200$ . The ground truth outlier matrix  $\mathbf{E}_{GT}$  is generated by selecting non-zero entries uniformly with probability  $\rho\in[0,1]$ , and its magnitudes are sampled iid from the uniform distribution  $U[-20,20]$ . We generate the ground truth low-rank matrix by  $\mathbf{Z}_{GT}=\mathbf{A}\mathbf{B}^\top$ , where  $\mathbf{A}\in\mathbb{R}^{n\times r}$  and  $\mathbf{B}\in\mathbb{R}^{m\times r}$  are drawn from iid  $\mathcal{N}(0,1)$ .

Figure 1 shows comparisons among competing methods, as well as the convex nuclear norm based matrix completion (CVX-MC) [6], the latter representing a *far easier* estimation task given that missing entry locations (analogous to corruptions) occur in known locations. The color of each cell encodes the percentage of success trials (out of 10 total) whereby the normalized root-mean-squared error (NRMSE,  $\frac{\|\hat{\mathbf{Z}}-\mathbf{Z}_{GT}\|_{\mathcal{F}}}{\|\mathbf{Z}_{GT}\|_{\mathcal{F}}}$ ) recovering  $\mathbf{Z}_{GT}$  is less than 0.001 to classify success following [5], [11].

Notably PB-RPCA displays a much broader recoverability region. This improvement is even maintained over TNN-RPCA and MC which require prior knowledge such as the true rank

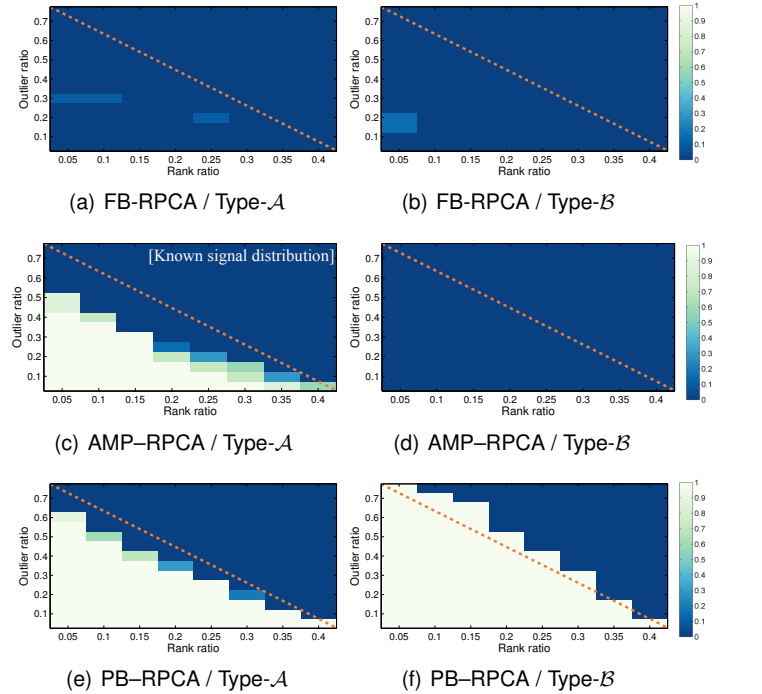


Fig. 2. Phase transitions of FB-RPCA [11], AMP-RPCA [28] and the proposed PB-RPCA by NRMSE over outlier (y-axis) and rank (x-axis) ratio variations for square matrix. This matrix size is used due to heavy computation of MCMC in FB-RPCA. All the experiment settings are consistent. Brighter color represents better performance.

and exact outlier locations respectively. These forms of prior knowledge offer a substantial advantage, although in practical situations are usually unavailable. PB-RPCA also outperforms PB-RPCA w/o sym. (its closest relative) by a wide margin, suggesting that the symmetry plays an important role. The poor performance of FB-RPCA is explained in the following.

For further analysis on FB-RPCA, we show additional phase transition graphs for FB-RPCA [11] in Fig. 2. Even though we applied the authors original code and settings, we observe that FB-RPCA seems to perform poorly with either the following data generation types:

- **Type-A:** Generate  $\mathbf{Z}_{GT}$  by  $\mathbf{Z}_{GT}=\mathbf{A}\mathbf{B}^\top$ , where  $\mathbf{A}\in\mathbb{R}^{n\times r}$  and  $\mathbf{B}\in\mathbb{R}^{m\times r}$  are drawn from i.i.d.  $\mathcal{N}(0,1)$ .  $\mathbf{E}_{GT}$  is drawn iid from  $U[-10,10]$ .

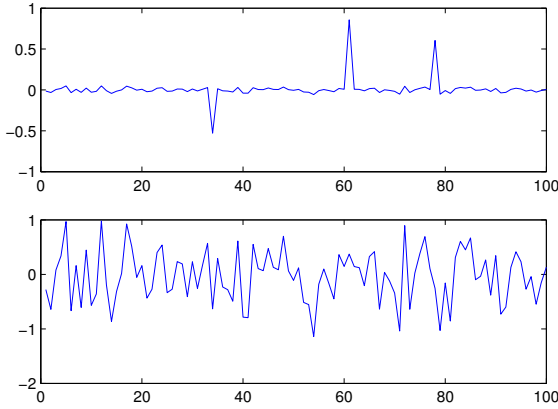


Fig. 3. Illustration of corrupted data samples. We plot a slice/column of a data matrix  $\mathbf{Y}$  generated by following [11] (top) and our Type- $\mathcal{A}$  scheme (bottom), and normalize them by maximum value for clear comparison. While the outlier locations are obvious in the top plot making the problem intrinsically easier, the Type- $\mathcal{A}$  data we generate (bottom) is not at all revealing. This makes the recovery problem far more difficult even though the effective SNR may actually be higher.

• **Type- $\mathcal{B}$ :** Generate  $\mathbf{Z}_{GT}$  and  $\mathbf{E}_{GT}$  by following Type- $\mathcal{A}$ , but  $\mathbf{A}$  and  $\mathbf{B}$  are drawn iid from the uniform distribution  $U[0, 1]$ .

Although a Gaussian distribution has conventionally been used to generate ground truth low-rank components (e.g., [5]), the singular value distribution of Type- $\mathcal{B}$  decays more rapidly and is more reflective of image data (e.g., a still image or video). Moreover, for PB-RPCA we found that performance actually increases with this data type (see Fig. 2); however, this is not the case for FB-RPCA.

The poor performance is likely because the Gibbs sampler becomes stuck in bad local optima given the challenging experimental conditions considered here. Note that even the simplest cell of the phase diagram, where the outlier ratio is 0.1 and the rank ratio is 0.05, is still far from a trivial setting to solve for FB-RPCA. However, this seems inconsistent with the quite impressive phase transition diagrams from [11], where superior performance relative to convex PCP is displayed in the main text.

Investigating further, we found that FB-RPCA seems to work best when the outliers have huge magnitudes relative to the low-rank component, i.e., the magnitudes of outliers sampled from  $U[-500, 500]$ .<sup>6</sup> Intuitively, if outliers have large values, their locations can be easily distinguished as illustrated in Fig. 3. Therefore, although the implicit SNR may be much lower, the actual estimation problem becomes much easier. In the more challenging conditions presented by our data generation scheme, we could not find any parameter setting such that FB-RPCA performed competitively. Note also that the algorithm is quite computationally intensive. Nonetheless, FB-RPCA still possesses some intrinsic advantages, such as the ability to learn diffuse noise parameters such as  $\lambda$ .

For comparison on AMP-RPCA, we use the same data generation scheme with either Type- $\mathcal{A}$  or - $\mathcal{B}$ , and show additional phase transition graph for AMP-RPCA [28] in Fig. 2-(c,d). With data generated by Type- $\mathcal{A}$ , AMP-RPCA works very well as shown in Fig. 2-(c). As mentioned in Section 2, the algorithm models data generation procedure with Gaussian distribution which is a consistent distribution with Type- $\mathcal{A}$ . However, with

6. This is proportionally similar to how the data was generated for the phase transition plots shown in [11].

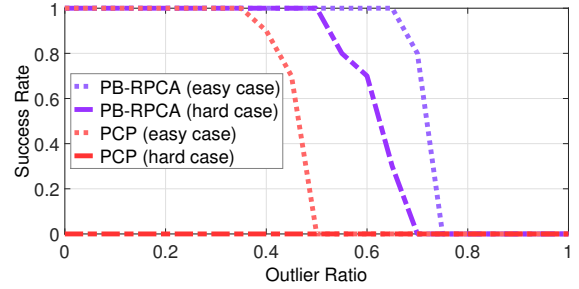


Fig. 4. Hard case comparison. The figure shows an interesting example for the hard case that PCP totally failed even in the low-rank and low outlier regime, while PB works quite stably. For the best view, refer to the electronic version.

| $\rho$  | SSC         | Robust SSC | PCP+SSC   | PB+SSC (Ours) |
|---|-------------|------------|-----------|---------------|
| Without sub-sampling (large number of measurements) |             |            |           |               |
| 0.1   | 19.0 / 14.9 | 5.3 / 0.3  | 3.0 / 0.0 | 2.4 / 0.0     |
| 0.2   | 28.2 / 28.3 | 6.4 / 0.4  | 3.0 / 0.0 | 2.4 / 0.0     |
| 0.3   | 33.2 / 34.7 | 7.2 / 0.5  | 3.6 / 0.2 | 2.8 / 0.0     |
| 0.4   | 36.5 / 39.0 | 8.5 / 0.6  | 4.7 / 0.2 | 3.1 / 0.0     |
| With sub-sampling (small number of measurements)    |             |            |           |               |
| 0.1   | 19.5 / 17.2 | 4.0 / 0.0  | 2.9 / 0.0 | 2.8 / 0.0     |
| 0.2   | 33.0 / 33.3 | 5.3 / 0.0  | 3.7 / 0.0 | 3.6 / 0.0     |
| 0.3   | 39.3 / 41.1 | 5.7 / 1.7  | 5.0 / 0.7 | 3.9 / 0.0     |
| 0.4   | 42.2 / 43.5 | 6.4 / 2.1  | 9.8 / 5.1 | 3.7 / 0.0     |

Fig. 5. Motion segmentation errors on Hopkins155. The parameter  $\rho$  denotes outlier ratio, and the numbers are miss classification rate in a format of {mean / median}.

Type- $\mathcal{B}$ , now there is a mismatch between the generative data distribution and that assumed by AMP-RPCA, and hence the algorithm is no longer competitive. In contrast, even with no prior information whatsoever, PB-RPCA nonetheless presents a stable phase transition curve with excellent performance.

**Hard Case Comparison:** Recovery of Gaussian iid low-rank components (the typical benchmark recovery problem in the literature) is somewhat ideal for existing algorithms like PCP because the singular vectors of  $\mathbf{Z}_{GT}$  will not resemble unit vectors that could be mistaken for sparse components. However, a simple test reveals just how brittle PCP is to deviations from the theoretically optimal regime. We generate a rank one  $\mathbf{Z}_{GT} = \sigma \mathbf{a}^3 (\mathbf{b}^3)^\top$ , where the cube operation is applied element-wise,  $\mathbf{a}$  and  $\mathbf{b}$  are vectors drawn iid from a unit sphere, and  $\sigma$  scales  $\mathbf{Z}_{GT}$  to unit variance.  $\mathbf{E}_{GT}$  has nonzero elements drawn iid from  $U[-1, 1]$ . Figure 4 shows the recovery results as the outlier ratio is increased. The *hard case* refers to the data just described, while the *easy case* follows the model used to make the phase transition plots. While PB-RPCA is quite stable, PCP completely fails for the hard data.

## 5.2 Outlier Removal for Motion Segmentation

Under an affine camera model, the stacked matrix consisting of feature point trajectories of  $k$  rigidly moving objects forms a union of  $k$  affine subspaces of at most rank  $4k$  [32]. But in practice, mismatches often occur due to occlusions or tracking algorithm limitations, and these introduce significant outliers into the feature motions such that the corresponding trajectory matrix may be at or near full rank. We adopt an experimental paradigm from [19] designed to test motion segmentation estimation in the presence of outliers. To mimic mismatches while retaining access to ground-truth, we randomly corrupt the entries of the trajectory matrix formed from Hopkins155 data [31]. Specifically, following [19] we add noise drawn

| No. Img. | LSQ [36] | PCP [37] | TNN [26] | Ours   |
|----------|----------|----------|----------|--------|
| 6        | 8.4138   | 21.1444  | 7.0961   | 6.6324 |
| 9        | 9.1616   | 11.6644  | 5.9152   | 5.5923 |
| 12       | 9.3569   | 10.7033  | 5.2036   | 4.4296 |
| 15       | 9.0895   | 9.8387   | 5.8332   | 4.1182 |

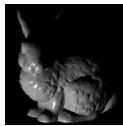


Fig. 6. Surface normal angular error (mean degree) on Bunny data (right-most).

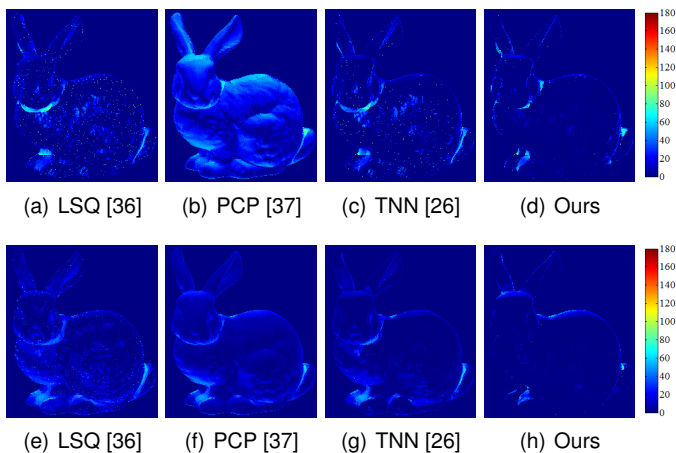


Fig. 7. Surface normal angular error map. The results are obtained from experiments with 6 (top) and 15 (bottom) input images. The unit of the error is degrees.

from  $\mathcal{N}(0, 0.1\kappa)$  to randomly sampled points with outlier ratio  $\rho \in [0, 1]$ , where  $\kappa$  is the maximum absolute value of the data. We may then attempt to recover a clean version from the corrupted measurements using RPCA as a preprocessing step; motion segmentation can then be applied using standard subspace clustering [32]. We use SSC and robust SSC algorithms [12] as baselines, and compare with RPCA preprocessing computed via PCP (as suggested in [12]) and PB-RPCA followed by SSC. Additionally, we sub-sampled the trajectory matrix to increase problem difficulty by fewer samples. Segmentation accuracy is reported in Fig. 5, where we observe that PB shows the best performance across different outlier ratios, and the performance gap widens when the measurements are scarce.

### 5.3 Outlier Removal for Uncalibrated Photometric Stereo

Photometric stereo is a method for estimating surface normals of an object or scene by capturing multiple images from a fixed viewpoint under different lighting conditions [36]. At a basic level, this methodology assumes a Lambertian object surface, point light sources at infinity, an orthographic camera view, and a linear sensor response function. Under these conditions, it has been shown that the intensities of a vectorized stack of images  $\mathbf{Y}$  can be expressed as

$$\mathbf{Y} = \mathbf{L}^T \mathbf{N} \mathbf{\Upsilon}, \quad (24)$$

where  $\mathbf{L}$  is a  $3 \times m$  matrix of  $m$  normalized lighting directions,  $\mathbf{N}$  is a  $3 \times n$  matrix of surface normals at  $n$  pixel locations, and  $\mathbf{\Upsilon}$  is a diagonal matrix of diffuse albedo values [36]. In general, the observed intensity matrix lies in a rank-3 subspace for Lambertian objects [14]. Thus, if we were to capture at least 3 images with known, linearly independent lighting directions we can solve for  $\mathbf{N}$  using least squares. Of course in reality many common non-Lambertian effects can disrupt this process, such as specularities, shadows, and image noise, etc. In many

cases, these effects can be modeled as an additive sparse error term  $\mathbf{S}$  applied to (24).

As proposed in [37], we can estimate the subspace containing  $\mathbf{N}$  by solving (1) assuming  $\mathbf{Z}^* = \mathbf{L}^T \mathbf{N} \mathbf{\Upsilon}$ . The resulting  $\hat{\mathbf{Z}}$ , combined with possibly other *a priori* information regarding the lighting directions  $\mathbf{L}$ , can lead to an estimate of  $\mathbf{N}$ . Since dealing with outliers via (24) does not require light information *a priori*, rank minimization approaches, such as [26], [37] and our method, are particularly beneficial for uncalibrated photometric stereo setups. In [37], a modified version of PCP is proposed for this task, where a shadow mask is included to simplify the sparse error correction problem. However, in practical situations, it may not always be possible to accurately locate all shadow regions in this manner, so it is desirable to treat them as unknown sparse corruptions. Note that in our experiment, we do not apply any preprocessing step like masking shadow or specular regions.<sup>7</sup>

We present an experiment to compare the performance of the standard least square method (LSQ) [36], PCP [37], TNN [26] and our proposed method, assuming that there is a good external method for surface normal recovery with unknown light directions. For each method, we estimate surface normals in a least squares manner given the ground-truth light direction information, after intensity observations are restored by PCP, TNN, and ours. LSQ is the baseline method without any restoration process.

Bunny data obtained from the Stanford 3D Scanning Repository<sup>8</sup> is used to generate photometric stereo data with known surface normals. Multiple 2D images with different known lighting conditions are easily generated using the Cook-Torrance reflectance model [10] to produce realistic specular effects as shown in Fig. 6. The average ratios of specular and shadow regions in the Bunny data are 8.4% and 24% respectively, which act as outliers. We add an additional 2% of random corruption outliers from  $U[0, 1]$ . These images are then stacked to produce  $\mathbf{Y}$ . We tested the algorithms as the number of images was varied with random lighting directions. The measured geometric surface normal errors are shown in Fig. 6, which are averaged across 10 trials. Recovered surface normal maps are displayed in Fig. 7.

A few things are worth highlighting with respect to these results. First, from a practical standpoint it is desirable to use fewer images for photometric stereo, and yet the underlying RPCA problem is decidedly more difficult in such cases. Interestingly, PCP is unable to outperform even the baseline LSQ in the difficult regime we tested with only 6 to 15 images and considerable outliers. The likely explanation is that the gap between solving (1) and (3) can be quite wide with insufficient data and equivalence conditions from [5] cannot be satisfied. Note however that if we do not account for biases in the outlier locations, LSQ may not always improve with additional images like all the RPCA methods eventually will. Overall though, our method consistently provides the most robust results with both limited and numerous images even without the benefit of additional prior knowledge (e.g., the target rank prior used by TNN).

<sup>7</sup> However, our method can naturally incorporate such a known mask when available by fixing variance parameters corresponding to missing entries to be large as described previously.

<sup>8</sup> <http://graphics.stanford.edu/data/3Dscanrep/>

## 6 CONCLUSION

Since the introduction of convex RPCA algorithms, there has not been a significant algorithmic break-through in terms of dramatically enhancing the regime where success is possible, at least in the absence of any prior information (beyond the generic low-rank and sparsity assumptions). The likely explanation is that essentially all of these approaches solve either a problem in the form of (4), an asymmetric problem in the form of (11), or else require strong priori knowledge. We provide a novel integration of three important design criteria, concavity, non-separability, and symmetry, that leads to state-of-the-art results by a wide margin *without tuning parameters or prior knowledge*.

## REFERENCES

- [1] S. D. Babacan, M. Luessi, R. Molina, and A. K. Katsaggelos. Sparse bayesian methods for low-rank matrix estimation. *IEEE Transactions on Signal Processing*, 60(8):3964–3977, 2012.
- [2] R. H. Bartels and G. Stewart. Solution of the matrix equation  $AX+XB=C$ . *Communications of the ACM*, 15(9):820–826, 1972.
- [3] C. M. Bishop. *Pattern recognition and machine learning*. Springer New York, 2006.
- [4] S. Boyd, N. Parikh, E. Chu, B. Peleato, and J. Eckstein. Distributed optimization and statistical learning via the alternating direction method of multipliers. *Foundations and Trends® in Machine Learning*, 2011.
- [5] E. J. Candès, X. Li, Y. Ma, and J. Wright. Robust principal component analysis? *Journal of the ACM (JACM)*, 58(3):11, 2011.
- [6] E. J. Candès and B. Recht. Exact matrix completion via convex optimization. *Foundations of Computational mathematics*, 9(6):717–772, 2009.
- [7] V. Chandrasekaran, S. Sanghavi, P. A. Parrilo, and A. S. Willsky. Rank-sparsity incoherence for matrix decomposition. *SIAM Journal on Optimization*, 21(2):572–596, 2011.
- [8] R. Chartrand. Nonconvex splitting for regularized low-rank+ sparse decomposition. *IEEE Transactions on Signal Processing*, 60(11):5810–5819, 2012.
- [9] Y.-L. Chen and C.-T. Hsu. A generalized low-rank appearance model for spatio-temporally correlated rain streaks. In *IEEE International Conference on Computer Vision (ICCV)*, pages 1968–1975, 2013.
- [10] R. L. Cook and K. E. Torrance. A reflectance model for computer graphics. *ACM Transactions on Graphics (SIGGRAPH)*, 1(1):7–24, 1982.
- [11] X. Ding, L. He, and L. Carin. Bayesian robust principal component analysis. *IEEE Transactions on Image Processing (TIP)*, 20(12):3419–3430, 2011.
- [12] E. Elhamifar and R. Vidal. Sparse subspace clustering: Algorithm, theory, and applications. *IEEE Transactions on Pattern Analysis and Machine Intelligence (TPAMI)*, 35(11):2765–2781, 2013.
- [13] J. Fan and R. Li. Variable selection via nonconcave penalized likelihood and its oracle properties. *Journal of the American Statistical Association*, 96(456):1348–1360, 2001.
- [14] H. Hayakawa. Photometric stereo under a light source with arbitrary motion. *Journal of the Optical Society of America A (JOSA)*, 11(11):3079–3089, 1994.
- [15] D. R. Hunter and K. Lange. A tutorial on MM algorithms. *The American Statistician*, 58(1):30–37, 2004.
- [16] H. Ji, C. Liu, Z. Shen, and Y. Xu. Robust video denoising using low rank matrix completion. In *IEEE Conference on Computer Vision and Pattern Recognition (CVPR)*, pages 1791–1798, 2010.
- [17] M. I. Jordan, Z. Ghahramani, T. S. Jaakkola, and L. K. Saul. An introduction to variational methods for graphical models. *Machine Learning*, 37(2):183–233, 1999.
- [18] Z. Lin, M. Chen, and Y. Ma. The augmented lagrange multiplier method for exact recovery of corrupted low-rank matrices. *arXiv:1009.5055*, 2010.
- [19] G. Liu and S. Yan. Latent low-rank representation for subspace segmentation and feature extraction. In *IEEE International Conference on Computer Vision (ICCV)*, pages 1615–1622, 2011.
- [20] C. Lu, Z. Lin, and S. Yan. Smoothed low rank and sparse matrix recovery by iteratively reweighted least squares minimization. *IEEE Transactions on Image Processing (TIP)*, 24(2):646–654, 2015.
- [21] K. Mohan and M. Fazel. Iterative reweighted algorithms for matrix rank minimization. *Journal of Machine Learning Research*, 13(Nov):3441–3473, 2012.
- [22] K. P. Murphy. *Machine Learning: a Probabilistic Perspective*. MIT Press, 2012.

- [23] K. P. Murphy, Y. Weiss, and M. I. Jordan. Loopy belief propagation for approximate inference: An empirical study. In *Conference on Uncertainty in Artificial Intelligence (UAI)*, pages 467–475, 1999.
- [24] T.-H. Oh, J.-Y. Lee, Y.-W. Tai, and I. S. Kweon. Robust high dynamic range imaging by rank minimization. *IEEE Transactions on Pattern Analysis and Machine Intelligence (TPAMI)*, 37(6):1219–1232, 2015.
- [25] T.-H. Oh, Y. Matsushita, I. S. Kweon, and D. Wipf. A pseudo-bayesian algorithm for robust PCA. In *Advances in Neural Information Processing Systems (NIPS)*, 2016.
- [26] T.-H. Oh, Y.-W. Tai, J.-C. Bazin, H. Kim, and I. S. Kweon. Partial sum minimization of singular values in Robust PCA: Algorithm and applications. *IEEE Transactions on Pattern Analysis and Machine Intelligence (TPAMI)*, 38(4):744–758, 2016.
- [27] J. A. Palmer. Relative convexity. *ECE Dept., UCSD, Tech. Rep.*, 2003.
- [28] J. T. Parker, P. Schniter, and V. Cevher. Bilinear generalized approximate message passing. *arXiv:1310.2632*, 2013.
- [29] Y. Peng, A. Ganesh, J. Wright, W. Xu, and Y. Ma. RASL: Robust alignment by sparse and low-rank decomposition for linearly correlated images. *IEEE Transactions on Pattern Analysis and Machine Intelligence (TPAMI)*, 34(11):2233–2246, 2012.
- [30] R. T. Rockafellar. *Convex analysis*. Princeton university press, 1970.
- [31] R. Tron and R. Vidal. A benchmark for the comparison of 3-d motion segmentation algorithms. In *IEEE Conference on Computer Vision and Pattern Recognition (CVPR)*, pages 1–8, 2007.
- [32] R. Vidal. Subspace clustering. *IEEE Signal Processing Magazine*, 28:52–68, 2011.
- [33] N. Wang and D.-Y. Yeung. Bayesian robust matrix factorization for image and video processing. In *IEEE International Conference on Computer Vision (ICCV)*, pages 1785–1792, 2013.
- [34] D. Wipf. Non-convex rank minimization via an empirical bayesian approach. In *Conference on Uncertainty in Artificial Intelligence (UAI)*, pages 914–923, 2012.
- [35] D. Wipf, B. D. Rao, and S. Nagarajan. Latent variable bayesian models for promoting sparsity. *IEEE Transaction on Information Theory*, 57(9):6236–6255, 2011.
- [36] R. Woodham. Photometric method for determining surface orientation from multiple images. *Optical Engineering*, 19(1):191139–191139, 1980.
- [37] L. Wu, A. Ganesh, B. Shi, Y. Matsushita, Y. Wang, and Y. Ma. Robust photometric stereo via low-rank matrix completion and recovery. In *Asian Conference on Computer Vision (ACCV)*, pages 703–717, 2010.
- [38] B. Xin and D. Wipf. Pushing the limits of affine rank minimization by adapting probabilistic PCA. In *International Conference on Machine Learning (ICML)*, pages 419–427, 2015.

## APPENDIX

### ADMM Subroutine for Updating $\mathbf{Z}$ and $\mathbf{E}$

We can obtain analytic solutions for  $\mathbf{Z}$  and  $\mathbf{E}$  using (16), but direct computation requires inversion of large matrices with complexity order  $O((nm)^3)$  which is often prohibitively expensive. Here we instead derive an efficient iterative approach for updating these variables to minimize the bound in (15). When  $\lambda \rightarrow 0$ , the data-dependent term converges to an equality constraint (the general case with  $\lambda > 0$  can also be dealt with as explained below). Then, the sub-problem for updating  $\mathbf{Z}$  and  $\mathbf{E}$  can be expressed as:

$$\min_{\mathbf{Z}, \mathbf{E}} \sum_{i,j} \frac{e_{ij}^2}{\gamma_{ij}} + \bar{\mathbf{z}}^\top \Sigma_{\bar{\mathbf{z}}}^{-1} \bar{\mathbf{z}} \quad \text{s.t. } \mathbf{Y} = \mathbf{Z} + \mathbf{E}, \quad (25)$$

where  $\Sigma_{\bar{\mathbf{z}}} \triangleq (\Psi_r \otimes \mathbf{I} + \mathbf{I} \otimes \Psi_c)$ . Since this sub-problem only consists of two smooth quadratic terms in  $\mathbf{Z}$  and  $\mathbf{E}$  and a linear equality constraint, it can be efficiently optimized using the alternating direction method of multipliers (ADMM) with guaranteed convergence [4].

The augmented Lagrange function is defined as

$$L_\mu(\mathbf{Z}, \mathbf{E}, \mathbf{Q}) = \sum_{i,j} \frac{e_{ij}^2}{\gamma_{ij}} + \bar{\mathbf{z}}^\top (\Psi_r \otimes \mathbf{I} + \mathbf{I} \otimes \Psi_c)^{-1} \bar{\mathbf{z}} \quad (26) \\ + \langle \mathbf{Q}, \mathbf{Y} - \mathbf{Z} - \mathbf{E} \rangle + \frac{\mu}{2} \|\mathbf{Y} - \mathbf{Z} - \mathbf{E}\|_{\mathcal{F}}^2,$$

where  $\mu$  is a positive scalar,  $\mathbf{Q} \in \mathbb{R}^{n \times m}$  is Lagrange multiplier, and  $\langle \cdot, \cdot \rangle$  represents the inner product operator. Now (26) can

**Algorithm 2** ADMM subroutine for updating  $\mathbf{Z}$  and  $\mathbf{E}$ .

**Input :** Observation matrix  $\mathbf{Y} \in \mathbb{R}^{n \times m}$ , stop criterion  $tol > 0$ , and  $\eta > 1$  (We set  $\eta = 1.5$ ).  
Initialize  $\mathbf{Q}_0 = \mathbf{0}$ ,  $\mu_0 > 0$  (We use  $\mu_0 = 1.25/\|\mathbf{Y}\|_2$ ).  
**repeat**  
  **repeat**  
    Update  $\mathbf{Z}$  by solving (29) and computing  $\Psi_c \mathbf{X} + \mathbf{X} \Psi_r$ .  
    Update  $\mathbf{E}$  using (27).  
  **until** Converged or reached at maximum number of iteration (We use 3 iterations).  
   $\mathbf{Q}_{k+1} = \mathbf{Q}_k + \mu_k(\mathbf{Y} - \mathbf{Z}_{k+1} - \mathbf{E}_{k+1})$ .  
   $\mu_{k+1} = \min(\mu_{\max}, \eta \mu_k)$ .  
**until**  $\max\left(\frac{\|\mathbf{Y} - \mathbf{Z}_{k+1} - \mathbf{E}_{k+1}\|_{\mathcal{F}}}{\|\mathbf{Y}\|_{\mathcal{F}}}, \frac{\|\mathbf{Z}_{k+1} - \mathbf{Z}_k\|_{\mathcal{F}}^2}{\mu_k \gamma_{ij}^2}\right) < tol$ .  
**Output :** Final estimate for  $\mathbf{Z}$  and  $\mathbf{E}$  for the subproblem (25).

be solved by minimizing each variable alternatively while fixing the others. Each  $e_{ij}$  can be updated using

$$e_{ij}^* = \arg \min_{e_{ij}} L_{\mu_k}(\mathbf{Z}_k, \mathbf{E}, \mathbf{Q}_k) = \frac{y_{ij} - z_{ij}^{(k)} + \mu_k^{-1} q_{ij}^{(k)}}{\frac{2}{\mu_k \gamma_{ij}} + 1}, \quad (27)$$

where  $k$  denotes the  $k$ -th iteration of ADMM. Also,  $\vec{z} = \text{vec}[\mathbf{Z}]$  can be updated via

$$\begin{aligned} \vec{z}^* &= \arg \min_{\vec{z}} L_{\mu_k}(\mathbf{Z}, \mathbf{E}_k, \mathbf{Q}_k) \\ &= \Sigma_{\vec{z}} (\Sigma_{\vec{z}} + 2\mu_k^{-1} \mathbf{I})^{-1} (\vec{y} - \vec{e}_k + \mu_k^{-1} \vec{q}_k). \end{aligned} \quad (28)$$

Even though this update does not yet reduce the computational complexity because of the required matrix inversion, we can nonetheless derive a very efficient update rule using (28) as follows.

Define the auxiliary variable  $\vec{x} \triangleq \Sigma_{\vec{z}}^{-1} \vec{z}^*$ . Then (28) is equivalent to solving the linear system  $(\Sigma_{\vec{z}} + 2\mu_k^{-1} \mathbf{I}) \vec{x} = \vec{b}$ , where  $\vec{b} = \text{vec}[\mathbf{B}] \triangleq (\vec{y} - \vec{e}_k + \mu_k^{-1} \vec{q}_k)$  is defined for convenience. We now observe that

$$\begin{aligned} (\Sigma_{\vec{z}} + 2\mu_k^{-1} \mathbf{I}) \vec{x} &= \vec{b} \\ \Rightarrow (\Psi_r \otimes \mathbf{I} + \mathbf{I} \otimes (\Psi_c + 2\mu_k^{-1} \mathbf{I})) \vec{x} &= \vec{b} \\ \Rightarrow (\Psi_c + 2\mu_k^{-1} \mathbf{I}) \mathbf{X} + \mathbf{X} \Psi_r &= \mathbf{B}. \end{aligned} \quad (29)$$

The last equation is derived from an identical form of Sylvester equation and can be efficiently solved with classical methods (e.g., the Bartels-Stewart algorithm [2] has complexity  $O(nm(n+m))$ , which is much less than the direct inversion requirement of  $O((nm)^3)$ ). In our experiments we use the Matlab built-in function, `sylvester`, to solve (29). After obtaining  $\mathbf{X}$ , we can compute the optimal solution  $\mathbf{Z}^*$  as  $\mathbf{Z}^* = \Psi_c \mathbf{X} + \mathbf{X} \Psi_r$ . The uniqueness of  $\mathbf{X}$  is guaranteed in this algorithm.

We follow the gradient update style rules for  $\mathbf{Q}$  as  $\mathbf{Q}_{k+1} = \mathbf{Q}_k + \mu_k(\mathbf{Y} - \mathbf{Z}_{k+1} - \mathbf{E}_{k+1})$  with  $\mu_{k+1} = \min(\mu_{\max}, \eta \mu_k)$ , where  $\eta > 1$ . The case where  $\lambda > 0$  can be handled by either setting a loose stop criterion for the fidelity term constraint. Therefore, we now have an efficient algorithm for updating  $\mathbf{Z}$  and  $\mathbf{E}$  as summarized in Algorithm 2.

**Proof of Proposition 2**

We begin with the first part of the proposition. Here we provide a basic sketch for brevity, but the launching point follows similar reasoning from [35, Theorem 4], which applies to related compressive sensing problems. In brief, using the dual-space

transformation from [35] and a few additional algebraic manipulations, in the limit as  $\lambda \rightarrow 0$ , then the global minimum of PB-RPCA under the stated conditions is equivalent to solving

$$\min_{\mathbf{Z}, \mathbf{E}} \frac{1}{2} [h_1(\mathbf{Z}, \mathbf{E}) + h_2(\mathbf{Z}, \mathbf{E})] \quad \text{s.t. } \mathbf{Y} = \mathbf{Z} + \mathbf{E}, \quad (30)$$

up to irrelevant scaling and translation factors, where we define

$$\begin{aligned} h_1(\mathbf{Z}, \mathbf{E}) &= \sum_i \text{rank}[\mathbf{Z}^\top \mathbf{Z} + \text{diag}(e_i)]^2 \\ h_2(\mathbf{Z}, \mathbf{E}) &= \sum_j \text{rank}[\mathbf{Z} \mathbf{Z}^\top + \text{diag}(e_j)]^2 \end{aligned} \quad (31)$$

and the squaring operator is understood to apply element-wise to rows and columns of  $\mathbf{E}$  respectively.

Let  $\{\mathbf{Z}', \mathbf{E}'\}$  denote the global solution to (1) which is unique by assumption. It then follows that any feasible solution to  $\mathbf{Y} = \mathbf{Z} + \mathbf{E}$  is such that  $h_1(\mathbf{Z}, \mathbf{E}) \geq n \text{rank}[\mathbf{Z}'] + \|\mathbf{E}'\|_0$  and  $h_2(\mathbf{Z}, \mathbf{E}) \geq n \text{rank}[\mathbf{Z}'] + \|\mathbf{E}'\|_0$ . To see this, let  $\mathbf{U}' \mathbf{S}' (\mathbf{V}')^\top$  denote the economy SVD of  $\mathbf{Z}'$  (meaning zero-valued diagonal elements of  $\mathbf{S}'$  are removed along with the corresponding columns of  $\mathbf{U}'$  and  $\mathbf{V}'$ ). If  $\{\mathbf{Z}', \mathbf{E}'\}$  truly represents the unique global optimum of (1), then any canonical coordinate vector (i.e., all zeros and a single one) of appropriate dimension cannot lie in the span of  $\mathbf{U}'$  or  $\mathbf{V}'$ , otherwise we could reduce  $\|\mathbf{E}'\|_0$  while holding  $\text{rank}[\mathbf{Z}']$  fixed.

Now suppose there exists a second feasible solution  $\{\mathbf{Z}'', \mathbf{E}''\}$  such that  $h_1(\mathbf{Z}'', \mathbf{E}'') < n \text{rank}[\mathbf{Z}'] + \|\mathbf{E}'\|_0$ , and let  $\mathbf{U}'' \mathbf{S}'' (\mathbf{V}'')^\top$  denote the corresponding economy SVD. This implies that  $\sum_i \text{rank}[(\mathbf{V}'')^\top (\mathbf{S}'')^2 \mathbf{V}'' + \text{diag}(e_i'')] < n \text{rank}[\mathbf{Z}'] + \|\mathbf{E}'\|_0$ . However, it is easily shown that such a solution will always exist such that  $\text{rank}[(\mathbf{V}'')^\top (\mathbf{S}'')^2 \mathbf{V}'' + \text{diag}(e_i'')] = \text{rank}[\mathbf{Z}'] + \|e_i''\|_0$  for all  $i$ . If this were not originally the case, we could simply adjust appropriate row-wise elements of  $\mathbf{E}''$  (associated with coordinate vectors in the span of  $\mathbf{V}''$ ) to zero such that this condition holds while maintaining feasibility. Therefore we arrive at a contradiction since by design we cannot have  $n \text{rank}[\mathbf{Z}'] + \|e_i''\|_0 < n \text{rank}[\mathbf{Z}'] + \|e_i'\|_0$ . And equivalent argument demonstrates that  $h_2(\mathbf{Z}, \mathbf{E}) \geq \text{rank}[\mathbf{Z}'] + \|\mathbf{E}'\|_0$ .

By the above reasoning, it follows that  $\{\mathbf{Z}', \mathbf{E}'\}$  must also be a global minimizer of (30); it only remains to show that this minimizer is unique. But this follows from the additional proposition conditions combined with the arguments above.

Regarding the second part of the proposition, it is sufficient to consider a simple demonstrative example. Let  $\Psi_c = \Psi_r = \epsilon \mathbf{I}$  for some  $\epsilon > 0$ . Then with  $\epsilon$  sufficiently small, a straightforward computation of the gradient of the objective (14) with respect to any  $\gamma_{ij}$  evaluated at  $\gamma_{ij} = 0$  is negative, indicating that we can obtain further reduction by increasing  $\gamma_{ij}$  from zero. While obviously this is just one particular example, it is emblematic of a much larger point: zero-valued coefficients  $\gamma_{ij}$  need not stay anchored at zero unlike with separable non-convex objectives under the stated conditions.  $\square$

**Connection with Convex PCP**

In this section, we introduce the theoretical relationship between the proposed method and convex PCP [5]. On the surface, it may appear that minimizing (14) is completely dissimilar to (3). However, a close relationship can be revealed by replacing the  $\log |\cdot|$  matrix operators in (14) with the trace operator  $\text{tr}[\cdot]$ . With just this simple substitution, we arrive at the modified cost function

$$\mathcal{L}'(\Psi_r, \Psi_c, \Gamma) \triangleq \vec{y}^\top \Sigma_y^{-1} \vec{y} + n \text{tr}[\Psi_c] + n \text{tr}[\Psi_r] + \|\Gamma\|_1, \quad (32)$$

noting that for simplicity we have assumed that  $n = m$  (i.e.,  $\mathbf{Y}$  is square); the general case can also be shown with some additional effort. We have also omitted irrelevant terms independent of  $\Psi_c$ ,  $\Psi_r$ , or  $\Gamma$ . This leads to the following:

**Proposition 3.** *The cost function (32) is convex over the domain of positive semi-definite, symmetric matrices  $\Psi_c$  and  $\Psi_r$ , and non-negative  $\Gamma$ . Furthermore, let  $\{\Psi_c^*, \Psi_r^*, \Gamma^*\}$  denote a globally minimizing solution and  $\{\mathbf{Z}^*, \mathbf{E}^*\}$  the associated values of  $\mathbf{Z}$  and  $\mathbf{E}$  computed using (16). Then  $\mathbf{Z}^*$  and  $\mathbf{E}^*$  also globally minimize*

$$\min_{\mathbf{Z}, \mathbf{E}} \frac{1}{2\lambda} \|\mathbf{Y} - \mathbf{Z} - \mathbf{E}\|_{\mathcal{F}}^2 + \sqrt{n} \|\mathbf{Z}\|_* + \|\mathbf{E}\|_1. \quad (36)$$

*Proof.* To begin we address the convexity of

$$\mathcal{L}'(\Psi_r, \Psi_c, \Gamma) \triangleq \bar{\mathbf{y}}^\top \Sigma_y^{-1} \bar{\mathbf{y}} + n \text{tr}[\Psi_c] + n \text{tr}[\Psi_r] + \|\Gamma\|_1. \quad (37)$$

Obviously, the trace and  $\ell_1$  norm terms are convex, so we only need consider the remaining  $\bar{\mathbf{y}}^\top \Sigma_y^{-1} \bar{\mathbf{y}}$  term. Since the function  $f(x) = g(\mathcal{A}(x))$  is convex if  $g$  is convex and  $\mathcal{A}$  is an affine function [30], in a same spirit, the remaining term can be re-expressed as

$$\begin{aligned} \bar{\mathbf{y}}^\top \Sigma_y^{-1} \bar{\mathbf{y}} &= \mathcal{A}_1(\mathbf{X}^{-1}), \\ \mathbf{X} &= \mathcal{A}_2(\Psi_c, \Psi_r, \Gamma). \end{aligned} \quad (38)$$

where  $\mathcal{A}_1$  and  $\mathcal{A}_2$  are affine functions. Obviously  $\mathcal{A}_1(\mathbf{X}^{-1})$  is a convex function of  $\mathbf{X}$  over the space of symmetric, positive definite  $\mathbf{X}$ . Moreover, composition with an affine function (or sum of affine functions) preserves convexity, hence by construction the overall function is convex in the respective arguments [30].

Moving forward, it can be shown that

$$\begin{aligned} \bar{\mathbf{y}}^\top \Sigma_y^{-1} \bar{\mathbf{y}} &= \min_{\mathbf{Z}_c, \mathbf{Z}_r, \mathbf{E}} \frac{1}{\lambda} \|\mathbf{Y} - \mathbf{Z}_c - \mathbf{Z}_r - \mathbf{E}\|_{\mathcal{F}}^2 + \sum_{i,j} \frac{e_{ij}^2}{\gamma_{ij}} \\ &\quad + \text{tr}[\mathbf{Z}_c^\top \Psi_c^{-1} \mathbf{Z}_c] + \text{tr}[\mathbf{Z}_r \Psi_r^{-1} \mathbf{Z}_r^\top]. \end{aligned} \quad (39)$$

Therefore minimizing  $\mathcal{L}'(\Psi_r, \Psi_c, \Gamma)$  is equivalent to solving

$$\begin{aligned} \min_{\Psi_c, \Psi_r, \Gamma, \mathbf{Z}_c, \mathbf{Z}_r, \mathbf{E}} \frac{1}{\lambda} \|\mathbf{Y} - \mathbf{Z}_c - \mathbf{Z}_r - \mathbf{E}\|_{\mathcal{F}}^2 + \sum_{i,j} \frac{e_{ij}^2}{\gamma_{ij}} \\ + \text{tr}[\mathbf{Z}_c^\top \Psi_c^{-1} \mathbf{Z}_c] + \text{tr}[\mathbf{Z}_r \Psi_r^{-1} \mathbf{Z}_r^\top] + n \text{tr}[\Psi_c] + n \text{tr}[\Psi_r] + \|\Gamma\|_1. \end{aligned} \quad (40)$$

This problem is jointly convex in  $\{\Psi_c, \Psi_r, \Gamma, \mathbf{Z}_c, \mathbf{Z}_r, \mathbf{E}\}$ . If we first optimize over  $\{\Psi_c, \Psi_r, \Gamma\}$  with  $\{\mathbf{Z}_c, \mathbf{Z}_r, \mathbf{E}\}$  fixed, it is easily demonstrated that the optimal solution is  $\Psi_c = (\frac{1}{n} \mathbf{Z}_c \mathbf{Z}_c^\top)^{1/2}$ ,  $\Psi_r = (\frac{1}{n} \mathbf{Z}_r \mathbf{Z}_r^\top)^{1/2}$ , and  $\gamma_{ij} = |e_{ij}|$  for all  $i, j$ . Plugging these values into (40), simplifying, and then applying the definitions of the nuclear and  $\ell_1$  norms, we arrive at the collapsed problem

$$\min_{\mathbf{Z}_c, \mathbf{Z}_r, \mathbf{E}} \frac{1}{2\lambda\sqrt{n}} \|\mathbf{Y} - \mathbf{Z}_c - \mathbf{Z}_r - \mathbf{E}\|_{\mathcal{F}}^2 + \|\mathbf{Z}_c\|_* + \|\mathbf{Z}_r\|_* + \frac{1}{\sqrt{n}} \|\mathbf{E}\|_1. \quad (41)$$

We may therefore conclude that minimizing values of (37), denoted  $\{\Psi_c^*, \Psi_r^*, \Gamma^*\}$ , must satisfy  $\Psi_c^* = [\frac{1}{n} \mathbf{Z}_c' (\mathbf{Z}_c')^\top]^{1/2}$ ,  $\Psi_r^* = [\frac{1}{n} (\mathbf{Z}_r')^\top \mathbf{Z}_r']^{1/2}$ , and  $\gamma_{ij}^* = |e'_{ij}|$  for all  $i, j$ , provided that  $\{\mathbf{Z}_c', \mathbf{Z}_r', \mathbf{E}'\}$  are optimal to (41). Additionally, by virtue of (39), if we optimize over  $\{\mathbf{Z}_c, \mathbf{Z}_r, \mathbf{E}\}$  with  $\{\Psi_c, \Psi_r, \Gamma\}$  fixed, the optimal solution is

$$\begin{aligned} \bar{\mathbf{z}}_c &= (\mathbf{I} \otimes \Psi_c) \Sigma_y^{-1} \bar{\mathbf{y}}, \\ \bar{\mathbf{z}}_r &= (\Psi_r \otimes \mathbf{I}) \Sigma_y^{-1} \bar{\mathbf{y}}, \\ \bar{\mathbf{e}} &= \bar{\Gamma} \Sigma_y^{-1} \bar{\mathbf{y}}, \end{aligned} \quad (42)$$

with  $\Sigma_y \triangleq \mathbf{I} \otimes \Psi_c + \Psi_r \otimes \mathbf{I} + \bar{\Gamma}$ . Consequently, at a globally optimal solution it must also hold that

$$\begin{aligned} \bar{\mathbf{z}}_c' &= (\mathbf{I} \otimes \Psi_c^*) (\Sigma_y^*)^{-1} \bar{\mathbf{y}}, \\ \bar{\mathbf{z}}_r' &= (\Psi_r^* \otimes \mathbf{I}) (\Sigma_y^*)^{-1} \bar{\mathbf{y}}, \\ \bar{\mathbf{e}}' &= \bar{\Gamma}' (\Sigma_y^*)^{-1} \bar{\mathbf{y}}, \end{aligned} \quad (43)$$

with  $\Sigma_y^* \triangleq \mathbf{I} \otimes \Psi_c^* + \Psi_r^* \otimes \mathbf{I} + \bar{\Gamma}'$ .

We now require an intermediate result:

**Lemma 1.** *Let  $\{\mathbf{Z}^*, \mathbf{E}^*\}$  denote the optimal solution to*

$$\min_{\mathbf{Z}, \mathbf{E}} \frac{1}{2\lambda\sqrt{n}} \|\mathbf{Y} - \mathbf{Z} - \mathbf{E}\|_{\mathcal{F}}^2 + \|\mathbf{Z}\|_* + \frac{1}{\sqrt{n}} \|\mathbf{E}\|_1. \quad (44)$$

*Then any  $\{\mathbf{Z}'_c, \mathbf{Z}'_r, \mathbf{E}'\}$  is optimal for (41) iff it satisfies*

$$\mathbf{Z}'_c + \mathbf{Z}'_r = \mathbf{Z}^*, \quad \mathbf{E}' = \mathbf{E}^*. \quad (45)$$

We omit the proof as it is rather straightforward after applying an SVD decomposition to  $\mathbf{Y}$  and noting the invariance of both the Frobenius and nuclear norms to orthogonal transforms.

We may now complete the proof as follows. If  $\{\Psi_c^*, \Psi_r^*, \Gamma^*\}$  minimizes (37), then  $\{\mathbf{Z}'_c, \mathbf{Z}'_r, \mathbf{E}'\}$  as specified via (43) must solve (41). However, if this is so, then  $\{\mathbf{Z}^* = \mathbf{Z}'_c + \mathbf{Z}'_r, \mathbf{E}^* = \mathbf{E}'\}$  must be optimal for (44). Given that

$$\begin{aligned} \bar{\mathbf{z}}^* &= \bar{\mathbf{z}}_c' + \bar{\mathbf{z}}_r' = (\mathbf{I} \otimes \Psi_c^* + \Psi_r^* \otimes \mathbf{I}) (\Sigma_y^*)^{-1} \bar{\mathbf{y}} \\ \bar{\mathbf{e}}^* &= \bar{\Gamma}^* (\Sigma_y^*)^{-1} \bar{\mathbf{y}}, \end{aligned} \quad (46)$$

the proof is completed.  $\square$

Interestingly, in the limit  $\lambda \rightarrow 0$ , (36) reduces to (3) with  $\alpha = \sqrt{n}$ , which is the exact same universal weighting factor theoretically motivated in [5] using complex Gaussian width arguments. Consequently, we may conclude based on Proposition 3 that convex RPCA is essentially equivalent to our method with the exception of the  $\text{tr}[\cdot]$  replacing  $\log|\cdot|$  in (14). This is somewhat remarkable considering how different these algorithms appear on the surface.

## VB-RPCA and Seperable Penalty Functions

On the surface, it may appear that VB-RPCA [1] is similar to the proposed PB-RPCA, both of which rely on probabilistic models; however, the former is quite different especially when viewed with respect to *Non-Separability* criteria from Section 4. But unfortunately the relationship between VB-RPCA and this non-separability property is significantly obfuscated. For example, the VB-RPCA algorithm invokes a variational free-energy-based cost function and then adopts a standard mean-field approximation as described in Section 2.

Interestingly however, we can show that this somewhat complicated inference procedure satisfies the following:

**Proposition 4.** *There exists some functions  $f_1$  and  $f_2$  such that all local (global) minima of (9) are in one-to-one correspondence with local (global) minima of (5). Additionally, if we track the means of  $q(\mathbf{Z})$  and  $q(\mathbf{E})$  during the coordinate descent minimization of (9), these updates are guaranteed to reduce or leave unchanged (5).*

*Proof.* Here we present the basic high-level proof. A few technical details common to VB algorithms are omitted for brevity. Solving

$$\min_{q(\Phi)} \mathcal{KL} [q(\Phi) \| p(\mathbf{A}, \mathbf{B}, \mathbf{E}, \Gamma, \theta | \mathbf{Y})] \quad (47)$$

$$\begin{aligned}
-2 \log p(\mathbf{A}, \mathbf{B}, \mathbf{E}, \Gamma, \theta, \mathbf{Y}) &\equiv \frac{1}{\lambda} \|\mathbf{Y} - \mathbf{A}\mathbf{B}^T - \mathbf{E}\|_{\mathcal{F}}^2 + \text{tr} \left[ \mathbf{A} \text{diag}[\theta]^{-1} \mathbf{A}^T + \mathbf{B} \text{diag}[\theta]^{-1} \mathbf{B}^T \right] \\
&+ (n+m) \sum_i \log \theta_i + \sum_{i,j} \left[ \frac{e_{ij}^2}{\gamma_{ij}} + \log \gamma_{ij} \right] - 2 \sum_{i,j} \log p(\gamma_{ij}) - 2 \sum_i \log p(\theta_i).
\end{aligned} \tag{33}$$

$$\begin{aligned}
&\min_{\bar{\mathbf{A}}, \bar{\mathbf{B}}, \bar{\mathbf{E}}, \Sigma_A, \Sigma_B, \Sigma_E} \frac{1}{\lambda} \left( \|\mathbf{Y} - \bar{\mathbf{A}}\bar{\mathbf{B}}^T - \bar{\mathbf{E}}\|_{\mathcal{F}}^2 + \text{tr} \left[ \bar{\mathbf{A}}^T \bar{\mathbf{A}} \Sigma_B \right] + \text{tr} \left[ \bar{\mathbf{B}}^T \bar{\mathbf{B}} \Sigma_A \right] + \text{tr} \left[ \Sigma_A \Sigma_B \right] \right) \\
&+ \frac{1}{\lambda} \sum_{i,j} (\Sigma_E)_{ij} + \text{tr} \left[ \left( \bar{\mathbf{A}}^T \bar{\mathbf{A}} + \Sigma_A \right) \mathbb{E}_{q(\theta)} \left( \text{diag}[\theta]^{-1} \right) \right] + \text{tr} \left[ \left( \bar{\mathbf{B}}^T \bar{\mathbf{B}} + \Sigma_B \right) \mathbb{E}_{q(\theta)} \left( \text{diag}[\theta]^{-1} \right) \right] \\
&+ \sum_{i,j} \left[ \bar{e}_{ij}^2 + (\Sigma_E)_{ij} \right] \mathbb{E}_{q(\gamma_{ij})} \left[ \gamma_{ij}^{-1} \right] + \log |\Sigma_A| + \log |\Sigma_B| + \sum_{i,j} \log [(\Sigma_E)_{ij}],
\end{aligned} \tag{34}$$

where  $\bar{\mathbf{A}}$ ,  $\bar{\mathbf{B}}$ , and  $\bar{\mathbf{E}}$  are arbitrary matrices of appropriate dimensions (representing posterior means),  $\Sigma_A$  and  $\Sigma_B$  are constrained to be positive semi-definite symmetric (such that the posterior expectations of  $\mathbf{A}^T \mathbf{A}$  and  $\mathbf{B}^T \mathbf{B}$  equal  $\bar{\mathbf{A}}^T \bar{\mathbf{A}} + \Sigma_A$  and  $\bar{\mathbf{B}}^T \bar{\mathbf{B}} + \Sigma_B$  respectively), and  $\Sigma_E$  is constrained only to have non-negative elements.

$$\begin{aligned}
&\min_{\bar{\mathbf{A}}, \bar{\mathbf{B}}, \bar{\mathbf{E}}, q(\theta), q(\Gamma)} \frac{1}{\lambda} \|\mathbf{Y} - \bar{\mathbf{A}}\bar{\mathbf{B}}^T - \bar{\mathbf{E}}\|_{\mathcal{F}}^2 + g_1(\bar{\mathbf{A}}, \bar{\mathbf{B}}; \mathbb{E}_{q(\theta)} [\text{diag}[\theta]^{-1}]) \\
&+ \sum_{ij} g_2(\bar{e}_{ij}; \mathbb{E}_{q(\gamma_{ij})} [\gamma_{ij}^{-1}]) - \mathbb{H}[q(\Gamma)q(\theta)].
\end{aligned} \tag{35}$$

TABLE 1  
Equations for proof of Proposition 4

is equivalent to minimizing the free energy defined by

$$\mathcal{F}[q(\Phi)] \triangleq \mathbb{E}_{q(\Phi)} [-\log p(\mathbf{A}, \mathbf{B}, \mathbf{E}, \Gamma, \theta, \mathbf{Y})] - \mathbb{H}[q(\Phi)], \tag{48}$$

where  $\mathbb{H}$  denotes the differential entropy and  $\mathbb{E}_{q(\Phi)}$  denotes expectation with respect to the distribution  $q(\Phi)$ . Based on the definitions of  $p(\mathbf{Y}|\mathbf{A}, \mathbf{B}, \mathbf{E})$ ,  $p(\mathbf{A}|\theta)$ ,  $p(\mathbf{B}|\theta)$ , and  $p(\mathbf{E}|\Gamma)$ , we also observe the negative log likelihood as (33, Table 1) with ignoring constant factors. Given the conjugate prior definitions and mean-field factorization of  $q(\Phi)$ , standard results from [3] dictate that  $\mathcal{F}[q(\Phi)]$  will be globally optimized when  $q(\mathbf{A})$ ,  $q(\mathbf{B})$ , and  $q(\mathbf{E})$  are Gaussian distributions. This implies that we may narrow optimization of these distributions to merely searching for optimal means and covariances without loss of generality. For the moment, assume that  $q(\Gamma)$  and  $q(\theta)$  are fixed. After some algebra, the resulting optimization over  $q(\mathbf{A})$  and  $q(\mathbf{B})$  then reduces to the equivalent problem (34, Table 1). Note that the log terms are based on the differential entropy of the associated Gaussian distributions. Because of how things have been decoupled, if we first optimize over  $\Sigma_A$ ,  $\Sigma_B$ , and  $\Sigma_E$ , then (34, Table 1) reduces further to

$$\begin{aligned}
&\min_{\bar{\mathbf{A}}, \bar{\mathbf{B}}, \bar{\mathbf{E}}} \frac{1}{\lambda} \|\mathbf{Y} - \bar{\mathbf{A}}\bar{\mathbf{B}}^T - \bar{\mathbf{E}}\|_{\mathcal{F}}^2 + g_1(\bar{\mathbf{A}}, \bar{\mathbf{B}}; \mathbb{E}_{q(\theta)} [\text{diag}[\theta]^{-1}]) \\
&+ \sum_{ij} g_2(\bar{e}_{ij}; \mathbb{E}_{q(\gamma_{ij})} [\gamma_{ij}^{-1}])
\end{aligned} \tag{49}$$

for some functions  $g_1$  and  $g_2$  (the exact form of these functions is not required for what follows). Returning to our original problem, solving (47) ultimately collapses to solving (35, Table 1). Finally, if we first optimize over  $q(\theta)$  and  $q(\Gamma)$ , we arrive at

$$\min_{\bar{\mathbf{A}}, \bar{\mathbf{B}}, \bar{\mathbf{E}}} \frac{1}{\lambda} \|\mathbf{Y} - \bar{\mathbf{A}}\bar{\mathbf{B}}^T - \bar{\mathbf{E}}\|_{\mathcal{F}}^2 + f_1(\bar{\mathbf{A}}, \bar{\mathbf{B}}) + \sum_{ij} f_2(\bar{e}_{ij}) \tag{50}$$

for some functions  $f_1$  and  $f_2$ . Moreover, if we define  $\mathbf{Z} = \bar{\mathbf{A}}\bar{\mathbf{B}}^T$  and  $\mathbf{E} = \bar{\mathbf{E}}$ , we observe that minimizing (47) is equivalent to solving (5) for some choice of  $f_1$  and  $f_2$ . The remaining points in the proposition statement follow directly from basic

properties of VB updates. Overall then, VB can be viewed as nothing more than a particular majorization-minimization algorithm [15] applied to solving a standard problem in the form of (5). Additionally, even though we have not provided a closed-form solution for the associated  $f_1$  and  $f_2$ , certain properties can nonetheless be analyzed, and there is no reason to believe that VB is exceptional in this regard.  $\square$

This is a quite surprising result, and it suggests that existing VB inference does not have any strong advantage over merely attacking (5) directly, except perhaps for computational efficiencies. In fact this problem is fundamental to any VB approach that relies on the factorization  $\mathbf{Z} = \mathbf{A}\mathbf{B}^T$  and then applies Gaussian scale-mixture hierarchical priors on  $\mathbf{A}$  and  $\mathbf{B}$  separately. Once this decision is made, and tractably solving (9) is accomplished using a  $q(\Phi)$  that factorizes over  $\mathbf{A}$ ,  $\mathbf{B}$ , and  $\mathbf{E}$ , then regardless of which specific scale-mixture is chosen, it will necessarily lead to the same conclusion as in Proposition 4.